DEFENCE R&D DÉFENSE

Graphical Investigation of Quantisation Effects of Phase Shifters on Array Patterns

Michel Clénet and Gilbert Morin
Defence Research Establishment Ottawa

Defence R&D Canada

DEFENCE RESEARCH ESTABLISHMENT OTTAWA

TECHNICAL REPORT
DREO TR 2000-092
November 2000

National Defence Défense nationale

Canada

Abstract

This document presents graphical investigations of the array factor of phased arrays with digital phase shifters. A software program based on basic antenna array theory has been developed in Matlab to obtain the main array characteristics (array factor and directivity). The array factors of linear arrays of different sizes with different types of phase shifters have been studied as a function of the number of bits and the frequency. Unconventional two-dimensional colour graphical representations are used to identify some characteristics of the array factor of arrays with digital phase shifters that can not be so clearly and quickly visualised with conventional graphical representations. Particularly, the effects of quantisation on the array factor for arrays of different sizes and for phase shifters with different numbers of bits, over scanning and frequency ranges, are shown using this representation. Numerous data are also provided.

Résumé

Ce document présente une étude graphique sur le facteur de réseau de réseaux a déphasage utilisant des déphaseurs numériques. Un programme base sur la théorie de base des réseaux d'antennes a été développé en langage Matlab, pour obtenir les principales caractéristiques des réseaux. Les facteurs de réseaux de réseaux linéaires de différentes tailles, et avec différents types de déphaseurs, ont été étudiés en fonction du nombre de bits du déphaseur et de la fréquence. Des représentations non conventionnelles, graphiques, couleurs et en deux dimensions sont utilisées pour identifier des caractéristiques des facteurs de réseau de réseaux alimentés avec des déphaseurs numériques, qui ne peuvent pas être si clairement et rapidement identifier avec des représentations graphiques conventionnelles. En particulier, les effets de la numérisation sur le facteur de réseau pour des réseaux de différentes tailles et pour des déphaseurs avec des nombres differents de bits, sont étudiées en utilisant cette représentation. De nombreuses données numériques sont également fournies.

Executive summary

With the advance of the technology digital phase shifters are nowadays widely used in phased array antennas to provide beam scan. The digital phase shifters deliver an approximated phase to steer the beam in the desired direction, whose approximation depends on the number of bits. The phase shift introduced by digitalisation generates also high-level side lobes, and decreases the directivity. In order to analyse the effect of phase digitalisation, studies on phased array antennas using digital phase shifter are carried out and are reported in this document. Linear arrays of point source radiating elements are considered, with different inter-element spacing and different number of elements. Investigations on the radiation characteristics are carried out versus the number of bits of the phase shifters, over scanning range and frequency range.

A code based on array antenna theory has been developed in Matlab. It allows studies of arrays of various geometrical shapes and lattices, associated with different kinds of phase shifters or with true-time delay lines. Using Matlab unconventional two-dimensional colour (2D-colour) graphic representations can be plotted, showing clearly and quickly some important characteristics that can not be directly observed with conventional graphic representations.

A first study, reported in Chapter 3, is conducted on the radiation characteristics of linear phased arrays, considering the number of bits of the phase shifters as parameter. With the help of 2D-colour plots, the study shows qualitatively that using digital phase shifters

- generates scan angle error,
- increases the side lobe levels,
- introduces additional high-level lobes,
- and as a consequence reduces the directivity.

These results are quantified for phased arrays of different sizes and with different number of bits, in order to determine the optimum number of bits considering a specific criterion. The study concludes that phase shifters with 3 or 4 bits, depending on the number of array elements, are satisfactory for most of the applications.

Array factor characteristics of linear phased arrays are investigated versus the inter-element spacing with the number of bits as parameter. Results are reported in Chapter 4. Studies are carried out considering, first, 25-element arrays with different inter-element spacing, and, second, arrays of fixed length with various inter-element spacing (and thus various number of elements). The effect of this parameter is clearly identified using 2D-colour graphic representations. The first study, conducted for different number of bits of the phase shifter, concludes that the radiation characteristics are not varying significantly throughout the scanning range. The second study shows that the scan angle error is slightly increasing with the increase of the inter-element spacing, while the other characteristics remain unchanged.

Results of array characteristics versus frequency are reported in Chapter 5. For this study linear arrays of 25-elements spaced by a half-wavelength are considered, associated to true-time delay lines, and to two kinds of phase shifters. The first kind, called constant-phase, delivers a constant phase over frequency, and the second kind, called switched-line, uses

switched lines (the length of the lines are estimated at a specific frequency). The required phase for each element is determined for a 30 GHz operating frequency and the study is carried out for a frequency range of 1 to 50 GHz. Using 2D-colour graphic representation, the effect of the frequency variations is clearly identified. Mathematical expressions are developed providing explanations on phenomena observed visually on the 2D-colour plots. This study concludes that best results are obtained with true-time delay lines, with which the scan angle remains constant over the frequency range. The use of constant-phase phase shifter introduced an unwanted frequency dependence of the scan angle, as well as the use of the switched-line phase shifters. The former is however preferred as no extra high-level lobes are generated unlikely the use of the latter.

This document presents investigations on phased arrays considering some characteristics of phase shifters, using a code developed for this purpose. This study is a first step in the study of phased arrays considering the characteristics of RF components, like phase shifters, true-time delay lines or amplifiers. This report shows particularly how colour graphic representations can help to extract important effects generated by different parameters of phased arrays.

Clénet. M. and Morin, G. A., 2000. Investigations on radiation characteristics of phased array antennas using digital phase shifters, DREO TR 2000-092, Defence Research Establishment Ottawa.

Sommaire

Avec l'avancée de la technologie, les déphaseurs numériques sont actuellement largement utilisés dans les réseaux à déphasage. Les déphaseurs numériques délivrent une valeur approchée de la phase requise pour pointer dans une direction privilégiée, et l'écart avec la valeur exacte dépend du nombre de bits. L'écart de phase introduit par la numérisation génère également une remontée du niveau des lobes secondaires et réduit la directivité. Afin d'analyser l'effet de la numérisation de la phase, des études portant sur les réseaux d'antennes à déphasage ont été menées et sont reportées dans ce document. Des réseaux linéaires constitués de points sources comme éléments rayonnants sont considérés, avec différents espacements entre les éléments et différents nombres d'éléments. Les études sur les caractéristiques de rayonnement sont conduites en fonction du nombre de bits du déphaseur, du secteur angulaire de balayage et de la bande frequencielle utile.

Un programme base sur la théorie des réseaux d'antennes a été développé en langage Matlab. Il permet l'étude de réseaux de forme géométrique quelconques, à treillis variés, associés à différents types de déphaseurs ou à des lignes à retard en vraie grandeur. En utilisant Matlab, des représentations graphiques non conventionnelles à deux dimensions (2D) en couleur peuvent être utilisées afin de visualiser clairement et rapidement quelques caractéristiques importantes qui ne pourraient être observées avec des représentations graphiques conventionnelles.

Une première étude, reportée au chapitre 3, est menée sur les caractéristiques de rayonnement de réseaux à déphasage linéaires, en considérant le nombre de bits du déphaseur comme paramètre. Avec l'aide de la représentation graphique 2D en couleur, cette étude montre qualitativement que l'utilisation de déphaseurs numériques

- génère une erreur de direction de pointage,
- élève le niveau des lobes secondaires,
- introduit des lobes de forte amplitude,
- réduit la directivité.

Ces résultats sont quantifiés pour des réseaux à déphasage de taille différente, en terme de nombre d'éléments, et pour des déphaseurs possédant un nombre de bits différent, afin de déterminer le nombre de bits optimum en considérant un critère particulier. L'étude conclue que les déphaseurs à 3 ou 4 bits sont satisfaisants pour la plupart des applications.

Les caractéristiques de réseaux à déphasage linéaires sont étudiés en fonction de l'espacement entre les éléments en considérant le nombre de bits des déphaseurs comme paramètre. Les résultats sont reportés au chapitre 4. Les études sont menées en considérant d'un part des réseaux de 25 éléments avec différentes distances inter-elements, et d'autre part des réseaux de longueur fixe avec différent espacement inter-elements (et donc un nombre différent d'éléments). L'effet de ce paramètre est clairement identifié en utilisant les représentations graphiques 2D en couleur. La première étude, réalisée pour différent nombre de bits du déphaseur, conduit à la conclusion que les caractéristiques de rayonnement ne sont pas perturbées de façon significative sur le secteur angulaire de balayage considéré. La deuxième étude montre que l'erreur de pointage augmente légèrement lorsque la distance entre les éléments augmente, alors que les autres caractéristiques restent inchangées.

Les résultats de la variation des caractéristiques de réseau en fonction de la fréquence sont reportés au chapitre 5. Pour cette étude, des réseaux linéaires de 25 éléments espacés d'une demi-longueur d'onde sont considérés, associés à des lignes à retard en vraie grandeur et à deux différents types de déphaseurs. Le premier type, appelé déphaseur à phase constante, délivre une phase constante sur toute la bande de fréquences considérée, alors que le deuxième type, dit à lignes commutées, utilise des longueurs de lignes commutées à l'aide d'interrupteurs (les longueurs de ligne sont estimées a une fréquence particulière). La phase requise pour chaque élément du réseau est déterminée à la fréquence de 30 GHz et l'étude porte sur une bande frequencielle allant de 1 a 50 GHz. L'effet de la fréquence sur le facteur de réseau est clairement identifié en utilisant les représentations graphiques 2D en couleur. Cette étude porte à conclure que les meilleurs résultats sont obtenus avec les lignes à retard de vraie grandeur, avec lesquelles la direction de pointage reste constante sur toute la bande de fréquences. L'utilisation de déphaseurs à phase constante conduit a une dépendance frequencielle de la direction de pointage, tout comme l'utilisation de déphaseurs à lignes commutées. Le premier type de déphaseurs est néanmoins préféré, car il n'introduit pas de lobes secondaires de forte amplitude.

Ce document présente des études sur les réseaux phases en considérant quelques caractéristiques des déphaseurs, réalisées en utilisant un programme développé dans ce but. Ces études constituent un premier pas dans l'étude de réseaux à déphasage en prenant en compte les caractéristiques de composants RF, comme les déphaseurs, lignes à retard ou les amplificateurs. Ce rapport montre également comment une représentation graphique en couleur peut permettre l'extraction d'effets importants générés par différents paramètres des réseaux à déphasage.

Clénet. M. and Morin, G. A., 2000. Investigations on radiation characteristics of phased array antennas using digital phase shifters. DREO TR 2000-92, Centre de recherches pour la défense Ottawa, DREO.

Table of contents

List of figures

List of tables

1 Introduction

Array antennas have been used for more than a half century. They received much more attention during the last two decades because of the extent of their utilisation in communication systems, especially for mobile and satellite communications. Digital phase shifters became preferred for such applications. The size of the phase shifter can be important, and is directly related to the number of bits, which is an important factor for the radiation performance of the array. This document reports investigation on the radiation characteristics of arrays incorporating digital phase shifters of different numbers of bits.

For this study linear arrays were considered. These arrays have different sizes in terms of numbers of elements and inter-element spacing. The array elements are point sources radiating in the upper half-space. Investigations on the radiation characteristics were carried out using scan and frequency ranges as parameters.

The results are reported in tables and figures. For figures, unconventional graphic representations are used. These graphs, which use colour scales, directly give an overall view of the array factor characteristics for a given configuration. They show clearly and quickly some characteristics that can not be detected with conventional graphic representations. The tables report the radiation characteristics averaged over a range of scan angles.

The first study, reported in Chapter 3, considered the effect of the number of phase shifter bits, as the radiation performance of the arrays depends strongly on this parameter. The investigations concern linear arrays with different numbers of elements, controlled by digital phase shifters with different numbers of bits. For comparison purposes the results of these arrays incorporating analogue phase shifters are also presented. By definition, an analogue phase shifter is a phase shifter which can deliver the exact phase to any array element of a phased array to steer the beam in the desired direction for a given frequency.

The subject of the second study, reported in Chapter 4, is the investigation of the array factor characteristics of arrays with different inter-element spacings. Digital phase shifters were used in these arrays. This study was divided into two parts. The first part concerned the results of 25-element arrays with inter-element spacings varying from a half-wavelength to a full wavelength. The second part reported the characteristics of 12-wavelength length arrays with inter-element spacings varying within the same range.

The last part of this report (Chapter 5) presented the study of the array factor characteristics versus frequency. A 25-element array was considered, fed by analogue and digital phase shifters. Arrays with constant-phase and switched-line phase shifters are compared to arrays using true-time-delay lines. This analysis clearly underlines advantages and drawbacks of each technique used to control phased array scanning.

But first of all, the program that has been developed in Matlab to carry out this study is described in Chapter 2. This program, called PAASoM standing for 'Phased array antenna software in Matlab', is based on basic array antenna theory. Although the results presented here are limited to linear phased arrays, the code is able to compute arrays of different geometries (linear, rectangular, triangular, hexagonal, octagonal, circular or others), and with different regular or irregular lattices (rectangular, triangular or hexagonal). Constant-phase phase shifters and switched-line phase shifters, analogue or digital with different numbers of bits, can be associated to each element, as well as true-time-delay feed systems. The results can be visualised with conventional two-dimensional graphs or with unconventional two-dimensional colour representation. This point is detailed in the following Chapter.

2 Description of the Phased Array Antenna Software in Matlab (PAASoM)

This chapter presents the description of a computer program developed in Matlab to analyse the radiation characteristics of phased arrays. This program is called PAASoM, standing for Phased Array Antenna Software in Matlab. Matlab has been chosen for its capability of data plotting and its multiple mathematical functions that are already defined.

The first part of this chapter gives an overview of the software. The second part describes the structure of the program, and finally the last part presents the output data.

2.1 Overview of the program

The software program PAASoM allows the studies of arrays of antenna elements of different geometries and lattices, and with the possibility of weighting each element in phase and magnitude. The array factor is calculated in one plane as a function of a parameter given by the user, such as the number of bits of the phase shifter, the scanning angle, the frequency or the azimuth angle indicating the plane of calculation.

The geometry can be read from a file that the user had previously created, or can be generated by the software. The geometries that can be generated are linear, rectangular, triangular, hexagonal, octagonal or circular (*Figure 1*). The elements of the array can be arranged in regular or irregular lattices. For regular lattices, the rectangular, triangular and hexagonal ones can be considered (*Figure 2*).

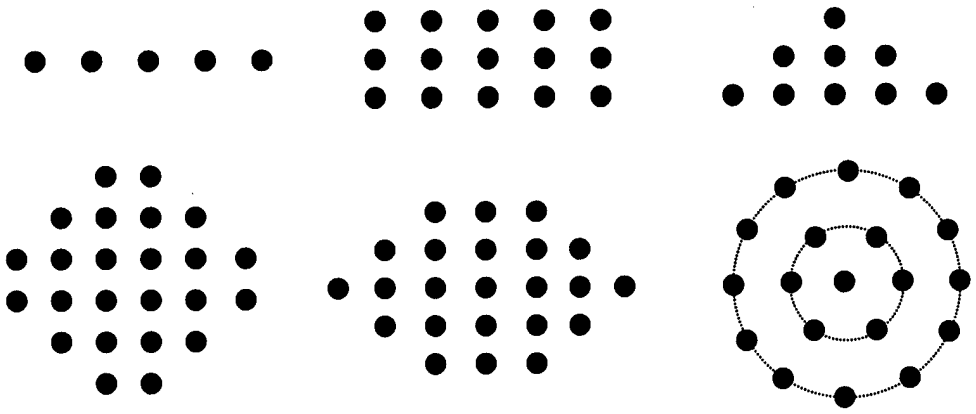

Figure 1: Array geometries generated with PAASoM

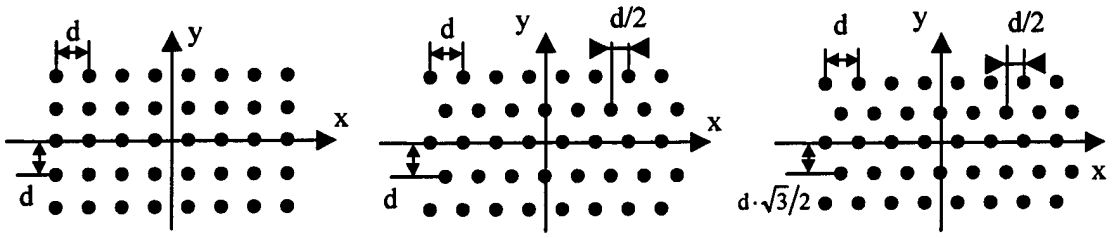

a) rectangular lattice b) triangular lattice c) hexagonal lattice

Figure 2: Lattices generated with PAASoM

Each antenna element can be fed through a phase shifter allowing the scan of the space. Different kinds of phase shifters can be considered. The first one is based on a constant phase concept. The phase for each element is determined at a specific frequency and remains constant over the frequency range of interest. If the phase shifter is digital the chosen phase is the closest one of the possible phase states. The second kind of phase shifter is based on a switched-line concept, and is directly related to MMIC (Microwave Monolithic Integrated Circuit) technology, which uses switches and lines of different lengths to obtain a set of phase steps. For example, a 3-bit switched-line phase shifter is shown in *Figure 3*.

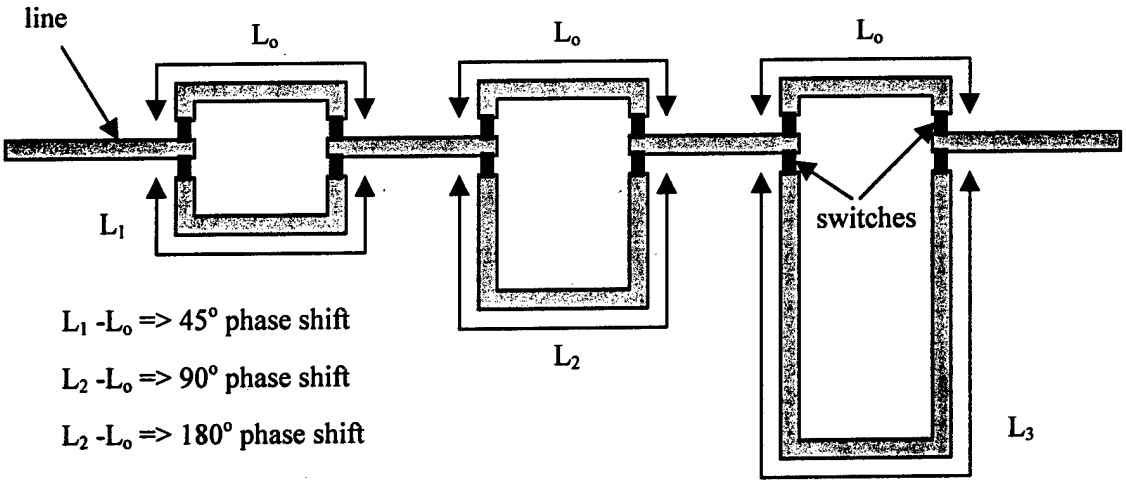

Figure 3: 3-bit switched-line phase shifter

In the case of switched-lines, the phase delivered to the element is expressed by:

$$\textit{(eq. 1)} \qquad \varphi_n = 2\pi f \tau_n \qquad \text{with} \qquad \tau_n = \frac{L_n}{c}$$

where

- φ_n is the phase delivered to the n^{th} element,
- τ_n is the delay for the n^{th} element,
- L_n is the length of the line selected for the n^{th} element,
- f is the frequency, and
- c is the speed of the light.

Considering the example presented in *Figure 3*, the phase delivered to the n^{th} element corresponds to the total length $L_n=b_1 (L_1 - L_0)+b_2 (L_2 - L_0)+b_3 (L_3 - L_0)$ where b_i is 0 or 1. Note that the maximum length of the line is a full wavelength at the frequency under consideration. The required phase is then modulus 2π.

Another method to steer the main beam has been implemented, based on the use of true delay lines for each element. In this case the length of the line required for the n^{th} element, expressed by *(eq. 2)*, is such that the corresponding phase is exactly the phase to scan in the desired direction. In other words, the phase is not restricted to the interval $[0;2\pi]$.

$$L_n = n\, d \sin(\theta_o) \qquad \textit{(eq. 2)}$$

where

- d is the inter-element spacing,
- θ_o is the scan angle

In its current version an amplitude distribution can be applied to the array. The pre-defined amplitude distributions are uniform, cosine of different power with or without pedestal, and Dolph-Chebyshev [1]. The latter can only be used for linear and rectangular arrays.

The kind of antenna element does not need to be specified, as the program computes the array factor (the array factor is the radiation pattern of the phased array based on point source elements). However, the program can take into account the radiation pattern of a specific antenna by reading an input file containing the amplitude of the electromagnetic field for the plane(s) of interest.

The parameters describing the characteristics of the phased array under consideration (geometry, lattice, kind of phase shifter and amplitude distribution) are put into an input file. Detailed information of the input file structure is given in *Annex 1*. The program computes the array factor from the input file. The structure of the software is discussed in the following section.

2.2 Structure of the program

This section presents the structure of the program. The computations of the array factor and the directivity are also developed.

The flow chart of the program is given in *Figure 4*. Each step is generated by a specific function called by the main program. The input and output data of each function are given in *Annex 2*.

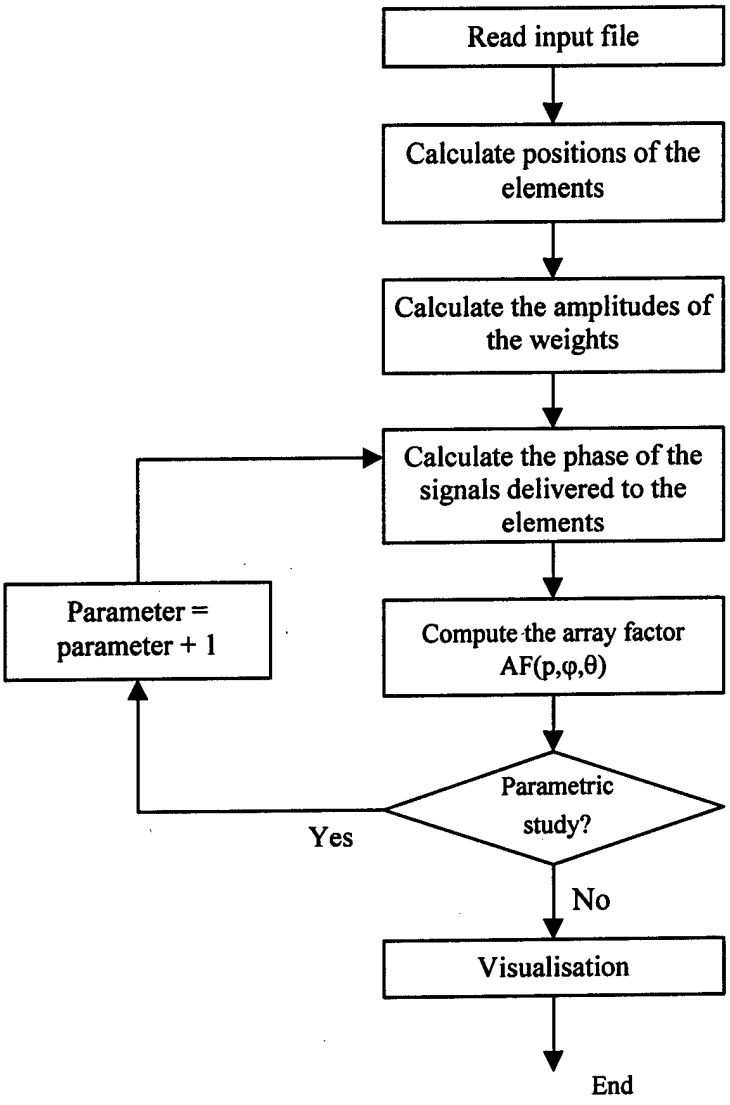

Figure 4: Flow chart of PAASoM

First, the software reads the input file containing the geometric parameters and the characteristics of the weighting (phase and amplitude). The input file also contains information needed to generate the output data. This point is discussed in the section *2.3*.

From the geometric parameters the position of each element is calculated, or read if specified by the user in the input file. The Cartesian co-ordinates of the elements are generated in a table of positions. This table is used afterwards with the input data of the chosen amplitude distribution to generate a vector of amplitudes. This vector defines the weightings of the antenna elements. Then, a table which contains the phase of each element is created from the corresponding input data and the array factor is finally computed. The phase and array factors are calculated again if a parametric study is desired. The parameter can be the number of bits of the phase shifter, the scanning angle, the frequency, or the plane of visualisation.

The array factor is calculated with the general equation:

$$AF(\theta,\varphi) = \frac{1}{M}\sum_{m=1}^{M} A_m e^{j\psi_m} e^{jk[x_m \cos(\varphi)\sin(\theta) + y_m \sin(\varphi)\sin(\theta) + z_n \cos(\theta)]} \qquad \textit{(eq. 3)}$$

where

- (x_m, y_m, z_m) are the Cartesian co-ordinates of the mth antenna element,
- (A_m, ψ_m) are respectively the amplitude and the magnitude of the weight of the mth antenna element,
- M is the number of antenna elements,
- (θ,φ) are the elevation and azimuth angles, as defined in *Figure 5*.
- k is the wave number,

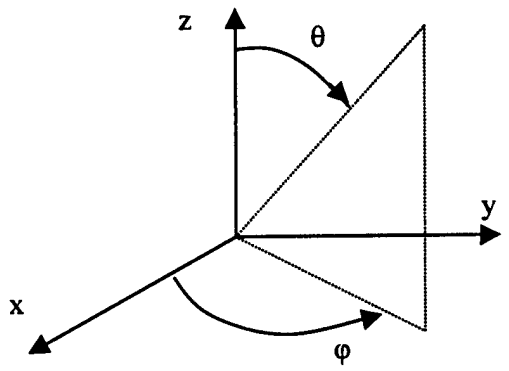

Figure 5: The spherical co-ordinate system

If indicated in the input file, some specific characteristics can be generated during the array factor computation as optional results. These include the maximum directivity, the side lobe positions and levels, the effective steering angle and the half-power beam width (HPBW). The

directivity is evaluated considering that the point-source antenna elements are radiating in the upper half-space. The expression is given by *(eq. 4)*.

$$\textbf{(eq. 4)} \qquad D(\theta,\varphi)=\frac{4\pi U(\theta,\varphi)}{P_{rad}}$$

where

$$U(\theta,\varphi)=\tfrac{1}{2\eta}\left|AF(\theta,\varphi)\right|^2$$

and

$$P_{rad}=\left[\frac{\pi}{N}\right]\left[\frac{2\pi}{M}\right]\sum_{j=1}^{M}\sum_{i=1}^{N}\frac{1}{2\eta}\left|AF(\theta_i,\varphi_j)\right|^2\sin(\theta_i)$$

with

$$\theta_i=\frac{\pi}{N}(i-1)-\frac{\pi}{2} \text{ and } \varphi_j=\frac{\pi}{M}(j-1)$$

The last step of the program is the presentation of the array factor (AF). Different kinds of graphs are possible. First, the common plot of the AF in one plane, called thereafter 2D-plot, can be generated. In the case of a parametric study, the different results are plotted in the same graphs, allowing direct comparison. The curves can be plotted in a Cartesian or polar co-ordinate systems. An example is shown in *Figure 6*, which shows plots of array factors with scan angle (θ_o) as a parameter.

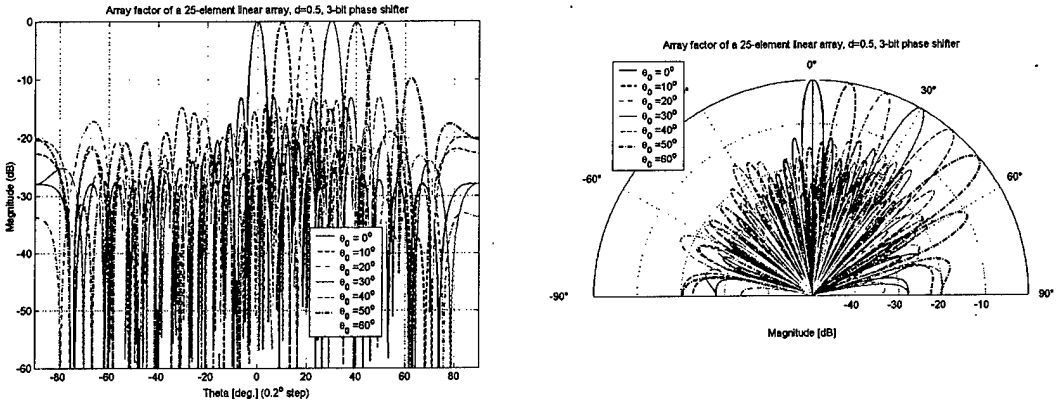

Figure 6: 2D Cartesian and polar representations of the array factors of a 25-element linear array with scan angle (θ_o) as parameter

A two-dimensional colour plot (2D-colour plot) is also possible in both co-ordinate systems. *Figure 7* gives an example. If the Cartesian co-ordinate system is selected, each horizontal line corresponds to the array factor calculated in one plane for a specific value of the defined parameter. In this case, *Figure 7a*, the array factor of a 25-element linear array is depicted in the main plane (horizontal axis) as a function of the scan angle (vertical axis). The colour indicates the magnitude in deciBels, and the colour scale is plotted in a colour bar on the right side of the graph. If the polar co-ordinate system is chosen, each half-circle corresponds to the AF in one plane for a specific value of the defined parameter, and the radius axis is the parameter. In this case, *Figure 7b*, the half-circle curves represent the AF in the main plane for one value of the parameter, and the radius depicts the value of the parameter, in this case the scan angle.

Figure 7a

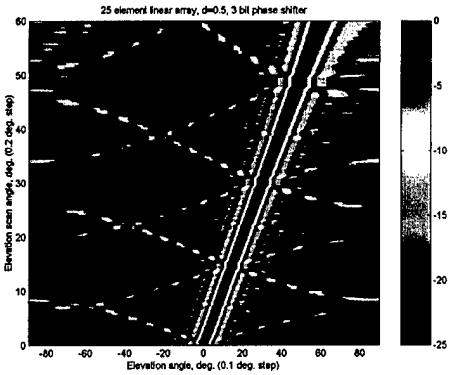

Figure 7b

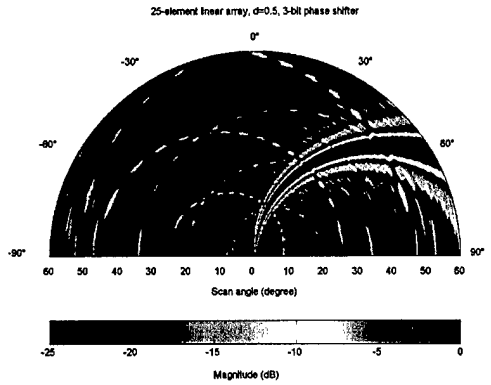

Figure 7: 2D-colour Cartesian and polar representations of the array factors of a 25-element linear array with scan angle as parameter

In most of the cases the horizontal axis in the Cartesian co-ordinate system, or angular co-ordinate in the polar co-ordinate system, is the elevation angle (θ) and the vertical axis, or radial axis, is the parameter. For such plots the graphs will be thereafter called:

- *elevation+scan* plot, if θ_o is the parameter,
- *elevation+frequency* plot if the frequency is the parameter,
- *elevation+azimuth* plot if φ is the parameter.

The optional results are given in text form. This point is discussed in the next section.

2.3 The output files

PAASoM writes output files of some data generated during the computation process. The table of element positions, and the amplitude and phase weights are saved in separated files. Note that the file for the phase contains a table of data corresponding to the phase of each

element for each value of the parameter. The names of these files correspond to the name of the input file followed by the truncated name of the data and terminated by the suffix ".dat". As an example, if the input filename is "test.txt", the filename

- "test_pos.dat" contains the Cartesian co-ordinates in wavelength of each antenna element,
- "test_ampl.dat" contains the amplitude of the weight of each antenna element,
- "test_phas.dat" contains the phase of the weight of each antenna element for each value of the parameter.

PAASoM also creates a file containing several radiation characteristics of the array under investigation, if the user requires these results. These data are: the desired scan angle, the maximum directivity, the obtained scan angle, the directivity in the direction of the desired scan angle, the half-power beam width of the main beam and the maximum side lobe level. The filename corresponds to the input filename with the suffix ".char".

To summarise, the program called PAASoM allows the study of the radiation characteristics of arrays, in terms of maximum directivity, array factor, position, width and level of the lobes. A lot of array geometry can be generated with PAASoM, with different lattices. The inter-element spacing can be regular or irregular. In addition the software can also read a file containing the Cartesian co-ordinates of the array elements. Several features are included:

- Each antenna element is fed through a digital or analogue phase shifter. The phase shifter can use the constant phase or constant delay concepts and is also characterised, if digital, by the number of bits.
- An amplitude weight can also be introduced for each antenna element by considering different distribution laws.
- Two kinds of graphs are possible, in both Cartesian and polar co-ordinate systems, allowing rapid and easy visualisation of the array factor.

Future versions of the software should contain more features. First, more amplitude distribution laws should be implemented. Models of phase shifters or amplitude weight generators should be taken into account from input files. The mutual coupling, which is an important factor in phased array studies, should be considered as well. Also, a three dimensional plot would be included, as the possibility of multiple graph generation. This list is non-exhaustive and depends on the future needs in phased array studies.

The following chapter presents some first results obtained with this software, on investigations of linear phased arrays.

3 Linear phased arrays with half wavelength inter-element spacing

This chapter concerns the investigations on directivity and array factor characteristics of linear phased arrays for different numbers of phase shifter bits.

In this chapter, the results for arrays with different numbers of elements are reported and analysed. For each array, phase shifters with 2 to 5 bits are considered. Three cases are fully described: 8-element array, 25-element array and 64-element array. Other arrays were investigated (from 8 to 128 elements) but only summarised data are reported, as the results are similar to those of the detailed studies.

3.1 Array configuration

The array configuration is shown in *Figure 8*. The elements are positioned on the horizontal axis. The inter-element spacing is chosen to be half a wavelength, to avoid grating lobes in the half space above the ground [2], pp29-33. The phase of the phase shifter for each element is chosen to be the closest one to the ideal phase to steer the main beam in the desired direction. As the study is for a single frequency the kind of phase shifter, constant-phased or switched-line, does not matter.

The array factors presented in this section are calculated for $-90^o \leq \theta \leq 90^o$ with a 0.2° step, and for $0^o \leq \theta_o \leq 60^o$ with a 0.2° step, unless otherwise noted. θ is the elevation angle and θ_o is the elevation scan or steering angle.

In addition, some average results over a scanning range are given to quantify array factor characteristics, like scan angle deviation, side lobe level or directivity loss. Unless otherwise noted, the average results mentioned in this chapter are calculated for $0^o \leq \theta_o \leq 60^o$ with a 1° step.

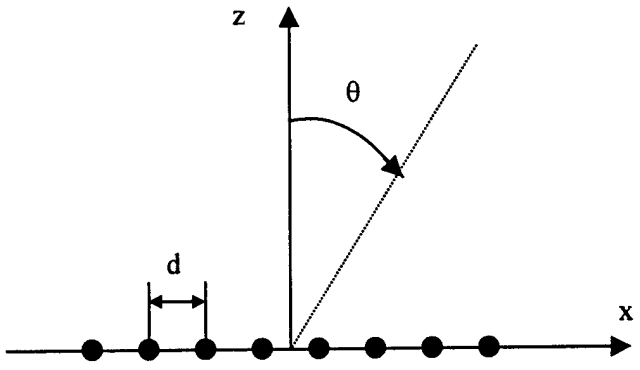

Figure 8: Linear array configuration

3.2 Eight element array

In order to estimate the discrepancies of the array factor characteristics due to the use of digital phase shifters, the array factor characteristics of an 8-element phased array with analogue phase shifters are first summarised. For the case of analogue phase shifters, each element is given the precise phase to scan in the θ_0 direction.

The maximum directivity for an array consisting of 8 point sources with a half-wavelength inter-element spacing radiating in the half-space is 11.99 dBi (for the directivity calculation, we consider that the array radiates only in the upper half-space). The directivity decreases with the increase of the scan angle following the *cos(θ)* law. For instance, the directivity drops to 8.98 dBi for a 60°-scan angle.

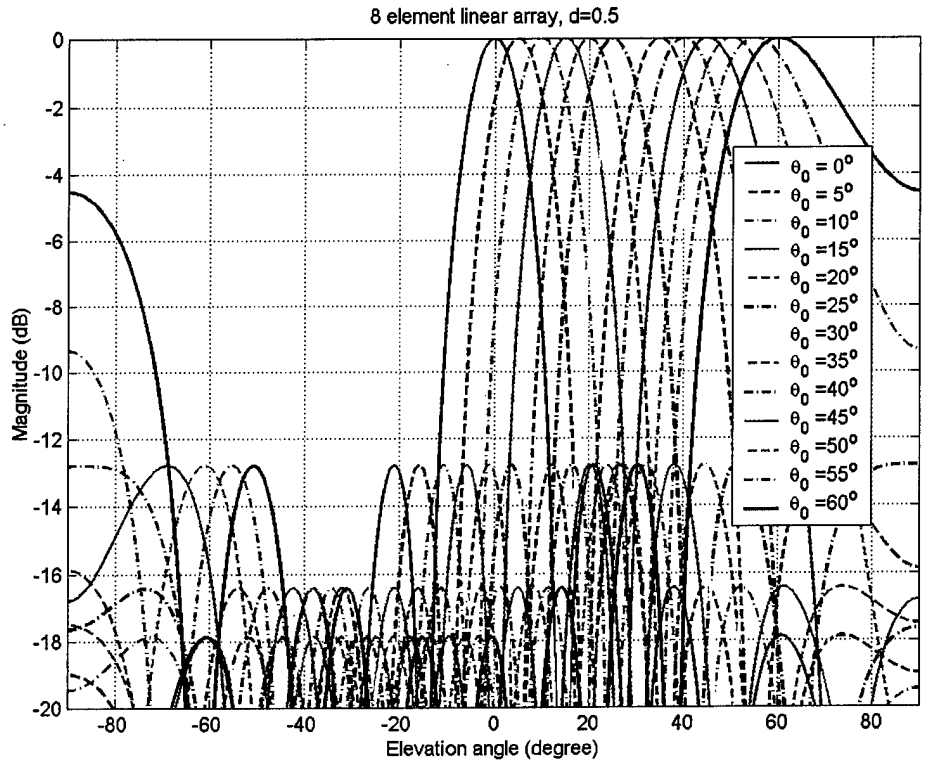

Figure 9: Array factor of an 8-element phased array with scan angle as parameter

Figure 9 shows the array factors in the main cut (plane containing the array) for a scan angle varying from 0° to 60° in 5° increments. The maximum side lobe level (max. SLL) is constant over the scanning range, and equals –12.8dB. The levels of the second and third SLLs are –16.5dB and –17.9dB, respectively. The half-power beam width (HPBW) increases as the main beam is scanned toward the horizon. In the broadside direction the HPBW is 12.8°, and it

slowly increases to reach 16.9° for θ_0=40° and 28.9° for θ_0=60°. The grating lobe rises to –9.2 dB for θ_0=55° and –4.3 dB for θ_0=60°.

Figure 10 gives another graphic representation of array factors. The graph shows the power of the radiated field for an elevation scan angle from 0° to 60° on the vertical axis and the elevation angle from –90° to 90° on the horizontal axis. For each elevation scan angle chosen (depicted on the vertical axis), the horizontal line through that value gives a plot of the array factor as a function of the elevation angle, with the magnitude of the array factor given by its colour. In such representation, it is easy to visualise the main lobe, side lobes, nulls and half-power beamwidth variations when the scan angle changes. Particularly, with the help of the black contour line at the –3 dB level, one can notice the widening of the HPBW with the increase of the scan angle. Also, the level of the grating lobe, visible in the top left corner of the figure, is higher than –10 dB for scan angles above 54°.

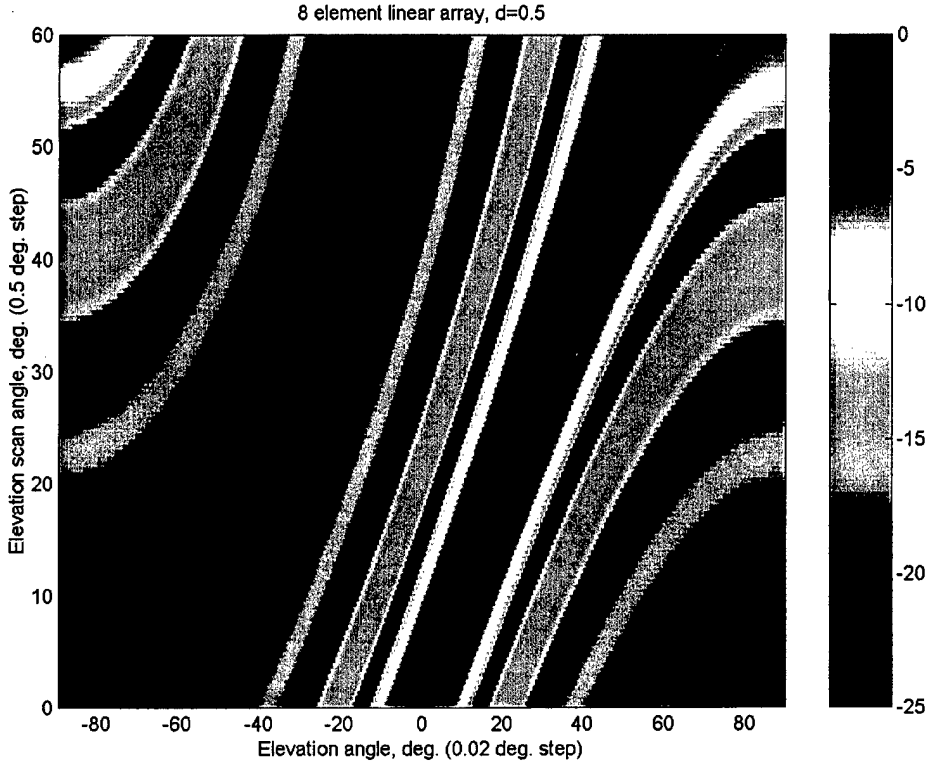

Figure 10: Array factor of an 8-element linear array, with analogue phase shifters versus scan angle (colour scale in dB)

3.2.1 One-bit phase shifter

With a 1-bit phase shifter, the phase is limited to two states: 0° and 180°. The maximum deviation from the phase required for each element to steer the beam in the desired direction is then 90°. This configuration leads to an important scan angle discrepancy. In addition, two simultaneous main lobes are generated as only two phase states are possible (0° and 180°). In other words, the array is not able to distinguish the left or the right sides. The additional main lobe is called quantisation lobe, and will be discussed in section *3.3*.

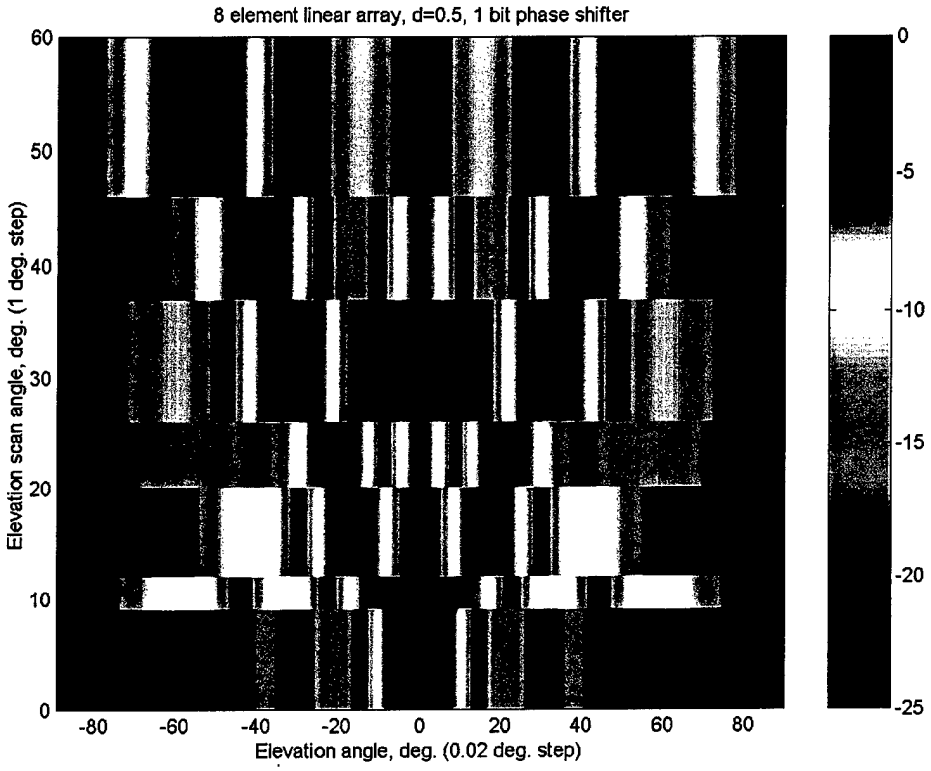

Figure 11: Array factor of an 8-element linear array, with 1-bit phase shifter versus scan angle (colour scale in dB)

Figure 11 shows the 2D-colour plot of the array factor in the main plane for a scan angle from –60° to 60° with 1° increments. The effect of phase quantisation appears clearly. The black line from (0,0) to (60,60) indicates the position of the array factor maximum for the desired scan angle.

Table 1 *Phase of the input of each element from 0° to 60° scan angle (radians)*

	ELEMENT NUMBER							
SCAN ANGLES	1	2	3	4	5	6	7	8
1: 0° to 9°	0	0	0	0	0	0	0	0
2: 9° to 12°	π	0	0	0	0	0	0	π
3: 12° to 20°	π	π	0	0	0	0	π	π
4: 20° to 26°	π	π	π	0	0	π	π	π
5: 26° to 37°	0	π	π	0	0	π	π	0
6: 37° to 46°	0	0	π	0	0	π	0	0
7: 46° to 60°	π	0	π	0	0	π	0	π

Only seven phase distributions are available to cover the 60°-scan range. From θ_o= 0° to 9° all the elements are in phase. Then, with the exception of those elements at the centre of the array, the phase of the elements changes as the scan angle changes. Note that the phase distribution of the array is symmetric about the centre line of the array. The various phase distributions are detailed in *Table 1*. Note that the maximum power can not be reached for θ_o>9° because of the presence of two main lobes located symmetrically with respect to the broadside direction.

3.2.2 Two-bit phase shifter

A 2-bit phase shifter provides 4 possible phase states: 0°, 90°, 180° and 270°. The maximum deviation from the phase required for each element to steer the beam in the desired direction is then 45°. The number of phase distributions in the 60°-scan angle range increases compared to the previous case, as shown in *Figure 12*.

The scan angle deviation is high for several steering angles. The obtained array factor does not change for scan angles from 21° to 30° (obtained scan angle is 25.4°), and another phase distribution gives the same pattern for a desired scan angle from 30.5° to 40.5° (obtained scan angle is 36.5°).

The signals radiated by each element are not optimally combined in the far field due to the limited number of phase states and therefore the result is that the side lobes do not appear at the same position and with the same power. Thus, the maximum side lobe level (SLL) is increased. As an example, the maximum SLL is –5.8 dB for $21^o \le \theta_o \le 40^o$, excluding θ_o near 30°. For $0^o \le \theta_o \le 60^o$ the maximum SLL fluctuates between –5.7 dB and –12.8 dB, and the average maximum SLL is –6.97 dB. This leads to 0.8 dB average drop of the maximum directivity with a 1.63 dB maximum drop for θ_o=30° (the average is calculated for $0^o \le \theta_o < 60^o$ with a 1° step from data printouts).

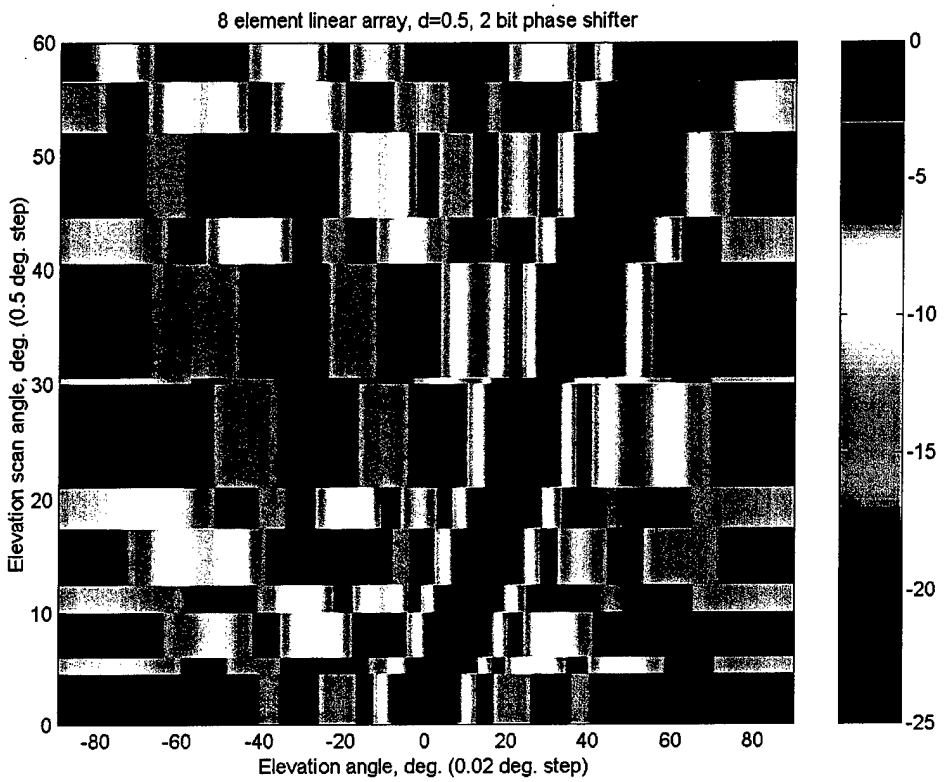

Figure 12: Array factor of an 8-element linear array, with 2-bit phase shifters versus scan angle (colour scale in dB)

3.2.3 Three-bit phase shifter

A 3-bit phase shifter gives eight possible phase states, starting at 0° with a 45° step. The maximum deviation of the phase of each element is then 22.5°. The scan angle error is considerably reduced compared to the case with the 2-bit phase shifter, as shown in *Figure 13*.

The patterns remain constant in the largest angular range for $43^o \le \theta_o < 49^o$, and for $49^o \le \theta_o < 55.5^o$. The maximum of 3.9° deviation occurs for θ_o=49°, while the average scan angle deviation over the scanning range, calculated for $0^o \le \theta_o < 60^o$ with a 0.5° step, is 1°. The average maximum SLL obtained with the 3-bit phase shifter is lower compared to the previous case (-10.2 dB), and varies along the scanning range from –8.9 dB to –12.8 dB (which is the maximum SLL in the broadside direction). The average directivity loss, calculated for $0^o \le \theta_o < 60^o$ with a 0.5° step, is 0.20 dB, with a 0.42 dB peak for θ_o=14.5°.

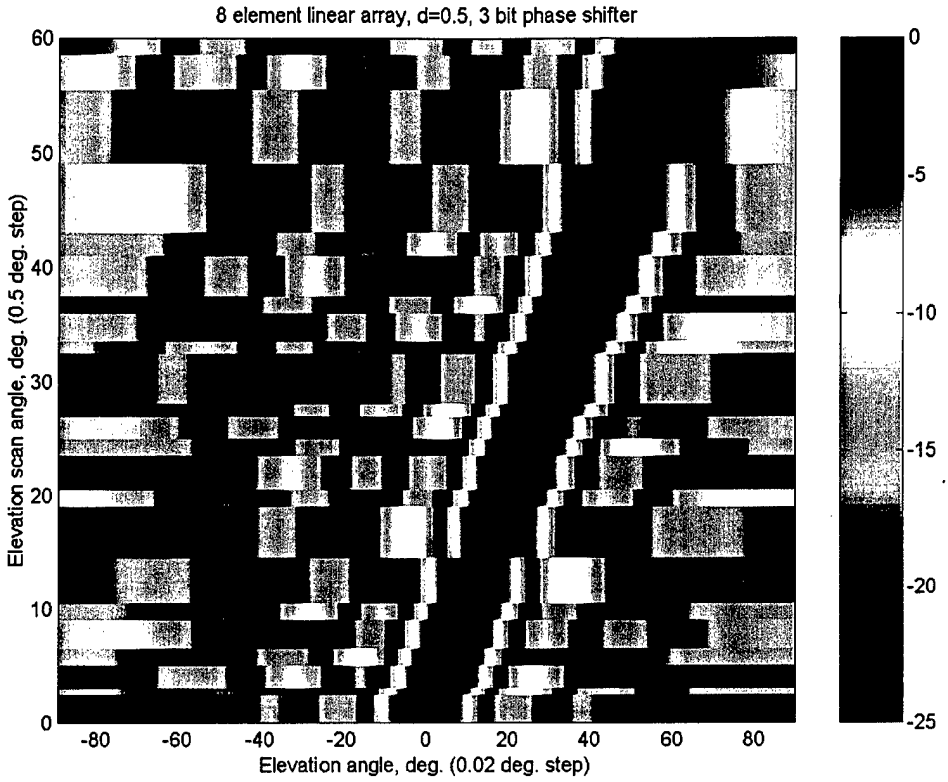

Figure 13: Array factor of an 8-element linear array, with 3-bit phase shifters versus scan angle (colour scale in dB)

Note that there is no scan angle deviation and no directivity loss for θ_o=30°. In this case the obtained phase distribution corresponds to the theoretical one, as the required phase for each element is a multiple of available phase states, i.e.,

$$kd\sin(\theta_o) = \pi/2 \qquad \textit{(eq. 5)}$$

Where:

- k is the wave number,
- d is the inter-element spacing,
- θ_o is the scan angle.

3.2.4 Four-bit phase shifter

16 phase states are possible with a 4-bit phase shifter, starting at 0° with 22.5° step. The maximum deviation of the phase of each element is now 11.25°. *Figure 14* shows the array factor in the *elevation+scan* representation.

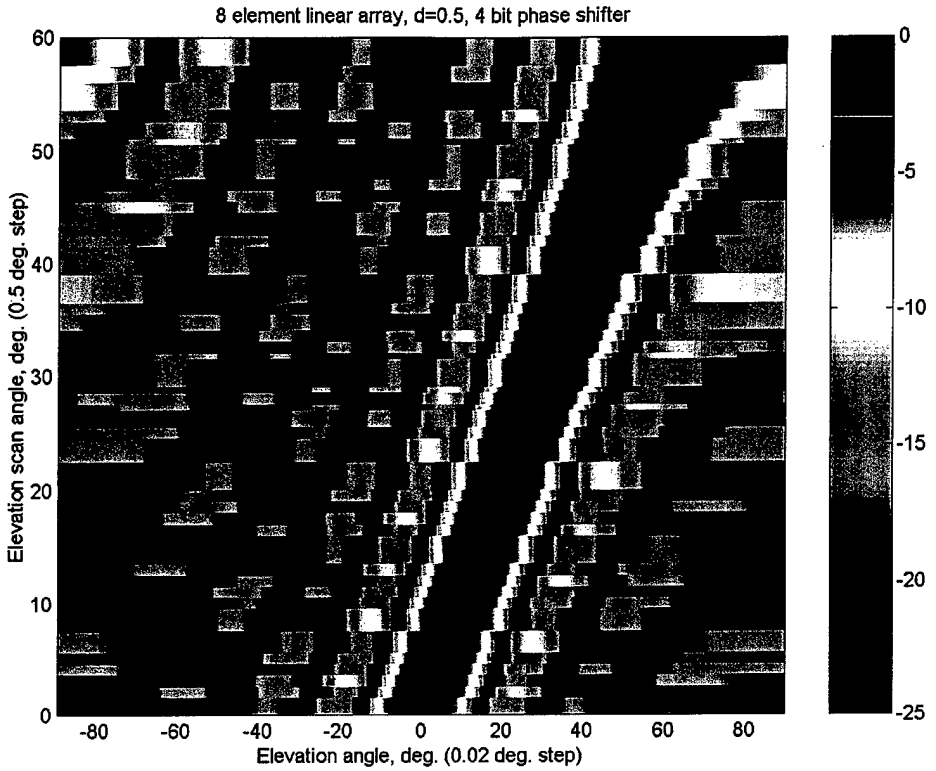

Figure 14: Array factor of an 8-element linear array, with 4-bit phase shifters versus scan angle (colour scale in dB)

The phase distributions are now changing more rapidly with the scan angle, following the theoretical pattern with less discrepancy. The maximum scan angle deviation occurs for θ_o=60° (1.66°), and the average scan angle deviation calculated for $0^{\circ} \le \theta_o < 60^{\circ}$ with a 0.5° step is 0.46°. The highest SLL equals –10.5 dB, and is reached around several scan angles (20°, 40°, 45° and 60°). The average directivity loss calculated for $0^{\circ} \le \theta_o < 60^{\circ}$ with a 0.5° step is lower than 0.05 dB with a maximum of 0.1 dB occurring at 22°. Again, with this array configuration (d/λ=0.5, where λ is the wavelength), ideal phase for the eight antenna elements can be obtained for θ_o=30°, and neither scan angle deviation nor directivity loss occur.

3.2.5 Five-bit phase shifter

Thirty-two phase states can be now used to steer the main beam. The maximum error of the phase required for each element is then 5.625°. This considerably reduces the scan angle deviation, as shown in *Figure 15*.

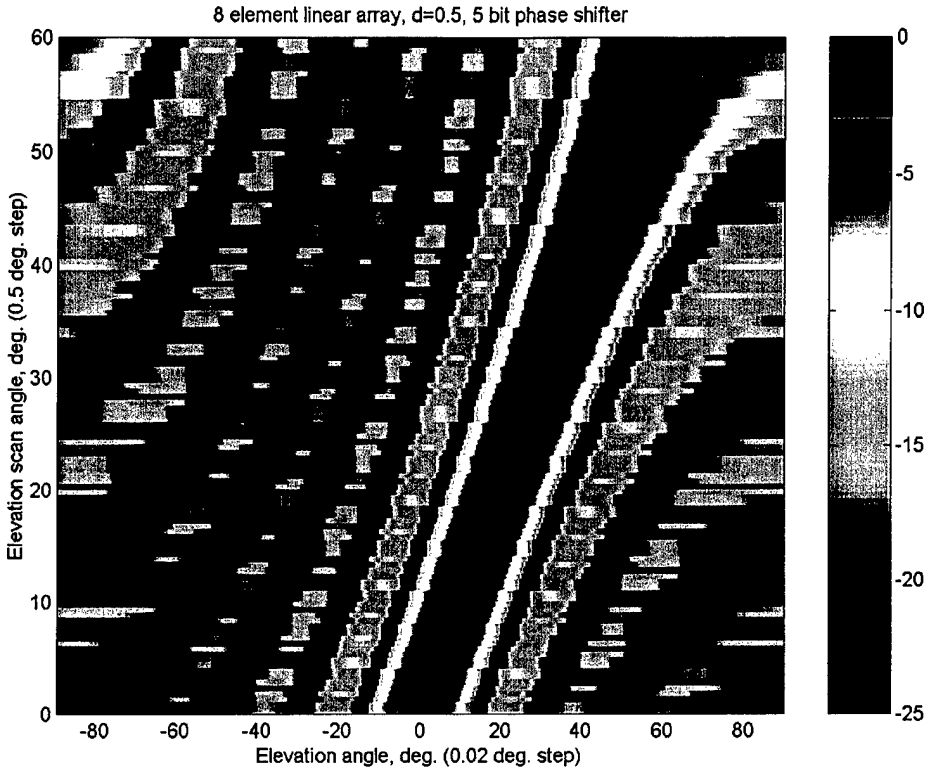

Figure 15: Array factor of an 8-element linear array, with 5-bit phase shifters versus scan angle (colour scale in dB)

The average scan angle deviation calculated for $0^o \leq \theta_o < 60^o$ with a 0.5° step is 0.23°, with a peak of 1° for θ_o=54.5°. The highest SLL equals –11.6 dB occurring for 6.5° and 60°. The directivity loss is now negligible with an average of 0.01 dB over the considered scanning range.

3.2.6 Concluding remarks

The study of the 8-element phased array with a half wavelength inter-element spacing gives a first idea about the effect of using digital phase shifters of different numbers of bits on the array factor characteristics. Due to the limited number of phase states, the scan angle is tilted, the side lobe level increases, and as a result the directivity decreases. However, increasing the number of bits sufficiently helps to obtain negligible scan angle deviation as well as directivity loss, as shown in *Figure 16* for a 35° scan angle.

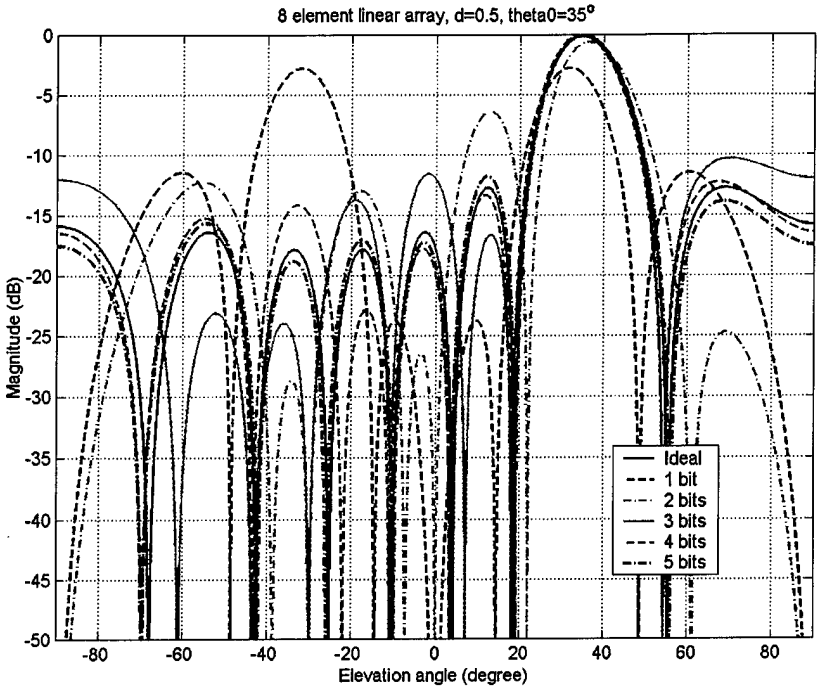

Figure 16: Array factor of an 8-element linear array for a 35°-scan angle

Table 2 summarises the average array factor characteristics for an eight element array utilising 1- to 5-bit phase shifters. Using a 4-bit phase shifter seems a good trade-off as the directivity loss drops to 0.05 dB, and the scan angle deviation relative to the HPBW is only 2.9%. For this specific case the average maximum SLL is acceptable (-11.6 dB).

Table 2 Average results of scan angle deviation, maximum SLL and directivity loss over scan angle for 8-element linear array using phase shifters of different numbers of bits

NUMBER OF BITS OF THE PHASE SHIFTER	1 BIT	2 BITS	3 BITS	4 BITS	5 BITS
Scan angle deviation, $\Delta\theta$ (deg.)	2.95	1.76	0.98	0.46	0.23
$\Delta\theta$ /HPBW (%)	18.89	11.34	5.98	2.87	1.42
Maximum SLL (dB)	-6.89	-6.97	-10.19	-11.62	-12.18
Directivity loss (dB)	3.15	0.82	0.20	0.047	0.012

The average is realised considering a scan angle varying from 0° to 60° with a 0.5° step.

The theoretical maximum SLL is -12.8 dB.

The array factor characteristics of an 8 element linear phased array with a half wavelength inter-element spacing have been fully described considering different number of bits for the phase shifter. However, an 8-element array is a relatively small array, and general analytic equations describing characteristics of large array can not be applied. Thus, we are going to study a 25-element phased array, in order to extend and generalise the different comments, and to compare our results to the theoretical results.

3.3 Arrays of 25 elements

The array factor characteristics of a 25 element array with a half wavelength inter-element spacing, considering 1- to 5-bit phase shifters are shown in *Figure 17b* to *Figure 17f*. They can be compared to *Figure 17a* which depicts the array factor obtained with an analogue phase shifter.

The maximum directivity of a 25-element array with analogue phase shifters radiating in the half-space is 16.94 dBi, occurring in the broadside direction. The HPBW is 4.1° for θ_o=0°, 5° for θ_o=35° and reaches 8.2° for θ_o=60°. The 1st side lobe level is -13.23 dB, approaching the –13.26 dB absolute maximum, obtained for an infinite array [3], p11. The second and the third SLL are –17.7 dB and –20.5 dB, respectively.

Figure 17b shows the array factor with the *elevation+scan* representation for the 25-element array with 1-bit phase shifter. Two main lobes occur as mentioned with the 8-element phased array. However, as the number of elements is increased, more phase distributions are possible and lead to reduce the scan angle deviation. The maximum phase deviation is 2° for θ_o=2°, and the average deviation calculated for $0^o \le \theta_o \le 60^o$ with a 1° step, is 0.46°. For the same condition, the average maximum SLL reaches –8.1 dB and the average directivity loss is 3.75 dB.

In this 2D-colour representation some curves appear with a mean level of about –10 dB, shown as light green curves. The curves are symmetric to the broadside direction, and start from the position (θ=0°, θ_o=0°), go to the position (θ=+/-90°, θ_o=20°), and then to the location (θ=+/-35°, θ_o=60°), crossing over at (θ=0°, θ_o=42°). These curves are due to quantisation lobes (QLs) which occur at specific positions depending on the scan angle, the number of array elements and the number of bits of the phase shifter [2]. The quantisation lobes can be evaluated in position and magnitude, [3], if the number of array elements is at least twice the number of phase states, i.e.,

$$N \ge 2^{M+1} \qquad \textit{(eq. 6)}$$

where:

- N is the number of elements of the array
- M is the number of bits.

In this case each phase step of the discrete phase distribution modifies at least the phase of two consecutive elements, and QLs will be produced as in a sub-array situation [3]. In fact, QLs can be considered as grating lobes produced by arraying sub-arrays of two or more

elements with spacing larger than a half wavelength. For a uniformly illuminated array, the scan angle deviation normalised to the array beamwidth is [4]:

$$\Delta\theta_o = \frac{\pi}{4}\frac{1}{2^M} \qquad \textit{(eq. 7)}$$

The magnitude of the first QL as a function of the number of bits is shown in *Table 3*.

Table 3 Magnitude of the first quantisation lobe (after [5])

NUMBER OF BITS OF THE PHASE SHIFTER	QL (dB)
2	-10.5
3	-17.1
4	-23.6
5	-29.8
6	-36.0

The quantisation lobes reduce the directivity, and the directivity loss can be approximated with [6]:

$$Loss \cong \sin c^2\left(\frac{\pi}{2^M}\right) \qquad \textit{(eq. 8)}$$

Results of directivity loss as a function of the number of bits are given in *Table 4*.

When the number of array elements is less than the number of phase steps, the discrete phase distribution has a random character. The average side lobe level due to the quantisation error is given as [4], [7]:

$$\sigma^2 = \frac{\pi^2}{3\cdot 2^{2M}}, \qquad \textit{(eq. 9)}$$

and the RMS side lobe level is σ^2/N. The directivity loss generated by the increased SLL is in first approximation:

$$Loss \cong 1-\sigma^2 \qquad \textit{(eq. 10)}$$

The directivity loss due to random phase errors is reported for different numbers of bits in *Table 4*. Note that these results are close to those obtained in the previous case.

Table 4 Directivity loss due to QL (after [5])

NUMBER OF PHASE SHIFTER BITS	REGULAR LOSS (dB)	RANDOM LOSS (dB)
2	0.912	1.000
3	0.224	0.229
4	0.056	0.056
5	0.014	0.014

One can also notice that the directivity losses obtained with an 8-element linear array (see *Table 2*, page 20) are in the same order. However, the QLs are not so visible on the 2D-colour representation graphs because the number of phase distributions is too small.

Figure 17c presents the array factor of the 25-element array with a 2-bit phase shifter. The first QL is easily visible with a magnitude -10.5 dB (yellow curves), and the second QL is also discernible (green curve) with a magnitude of –14.9 dB [3], p30. The maximum phase deviation is 1° for θ_o=1° and θ_o=31°, and the average scan angle deviation calculated for $0^o \leq \theta_o \leq 60^o$ with a 1° step, is 0.26°. For the same condition, the average directivity loss is 0.84 dB and the average maximum SLL reaches –9.2 dB.

The array factors of the 25 element array with a 3-bit phase shifter is shown in *Figure 17d.* Once again the quantisation lobes occur but with a lower magnitude (-17 dB, dashed green curves). The average maximum side lobe level drops to –12.1 dB, and the average directivity loss decreases to 0.21 dB with a maximum of 0.27 dB at θ_o=27°. The average scan angle deviation decreases to 0.15° compared to that of the array with 2-bit phase shifter.

Figure 17a

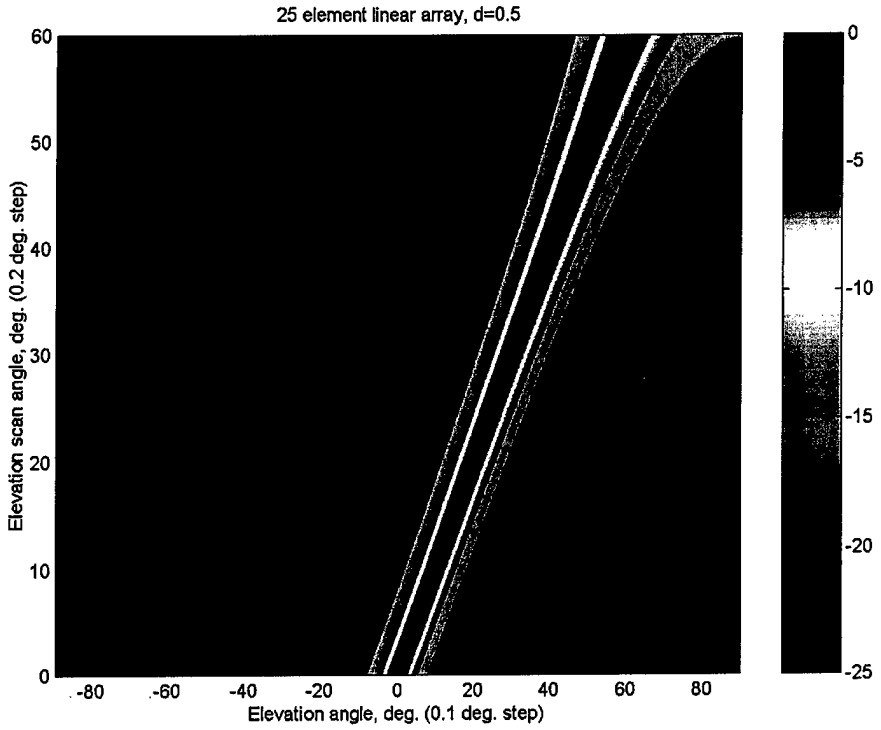

Figure 17b

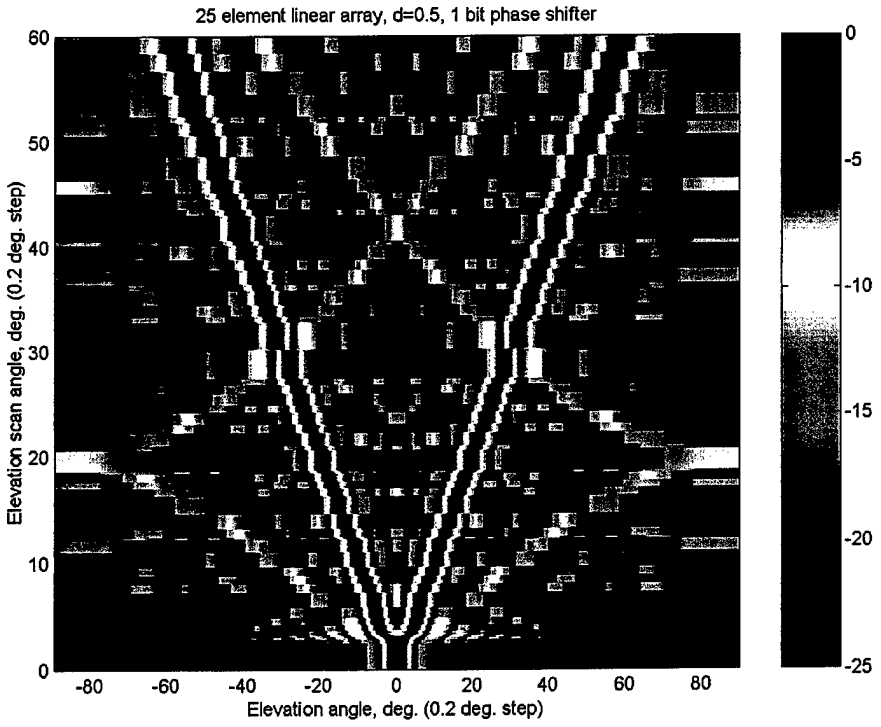

Figure 17c

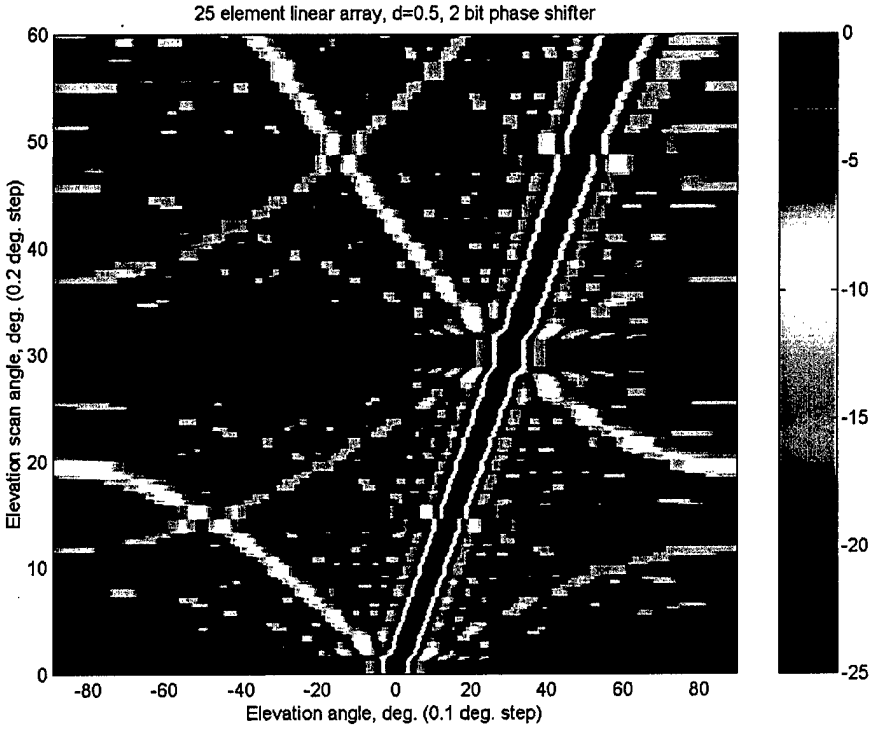

Figure 17d

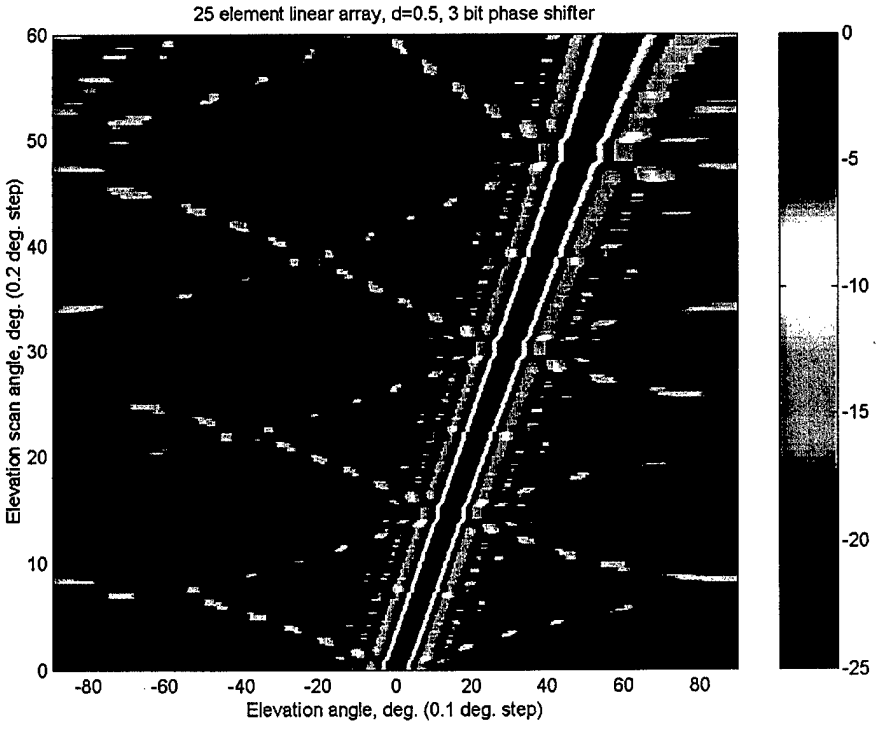

Figure 17e

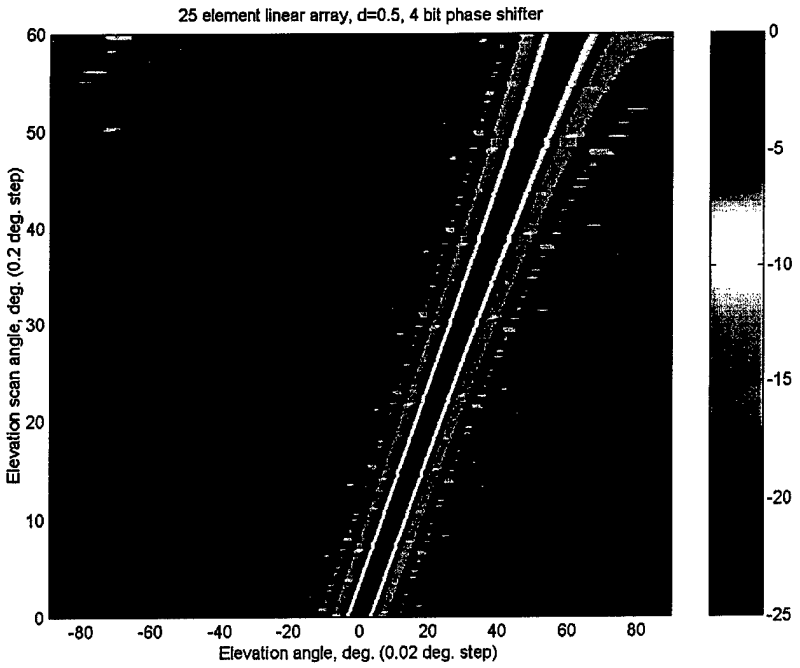

Figure 17f

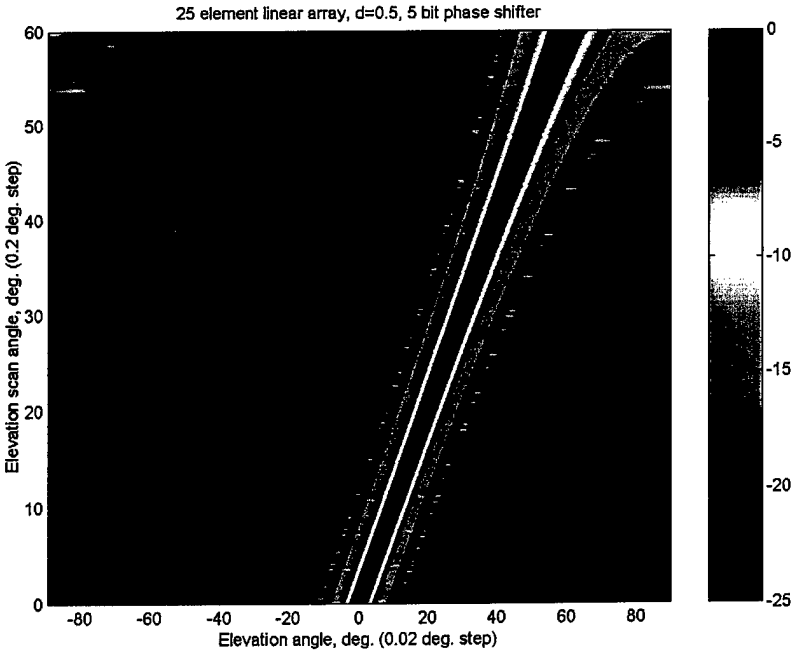

Figure 17: Array factor of a 25-element linear phased array with different phase shifters; a) analogue, b) 1-bit, c) 2-bit, d) 3-bit, e) 4-bit, f)-5bit (colour scale in dB)

The magnitude of the quantisation lobes decreases as the number of bits increases, as shown in *Figure 17e* and in *Figure 17f*. They are hardly discernible from 5 bits because of the use of the 25 dB colour scale. The QL levels are higher than indicated in *Table 3*, because they now behave randomly as the number of array elements is lower than the number of phase steps. The SLLs rise slightly, but the levels are lower than –12.6 dB for both cases. Also, the average directivity losses are lower than 0.1 dB for 4 and 5 bits, and the average scan angle deviations normalised to the HPBW are 1.26% and 0.52%, respectively.

Figure 18 gives the array factors of the 25 element array with 1 to 5-bit phase shifters for a 35° scan angle in the θ=0° plane. For this particular steering angle, the first quantisation lobe is easily observed, appearing at θ=-35° for 1 bit, θ=59° for 2 bits, θ=-57° for 3 bits and θ=-36° for 4 bits. With the 5-bit phase shifters, the QLs can not be distinguished from the side lobes of the array factor of the 25-element array.

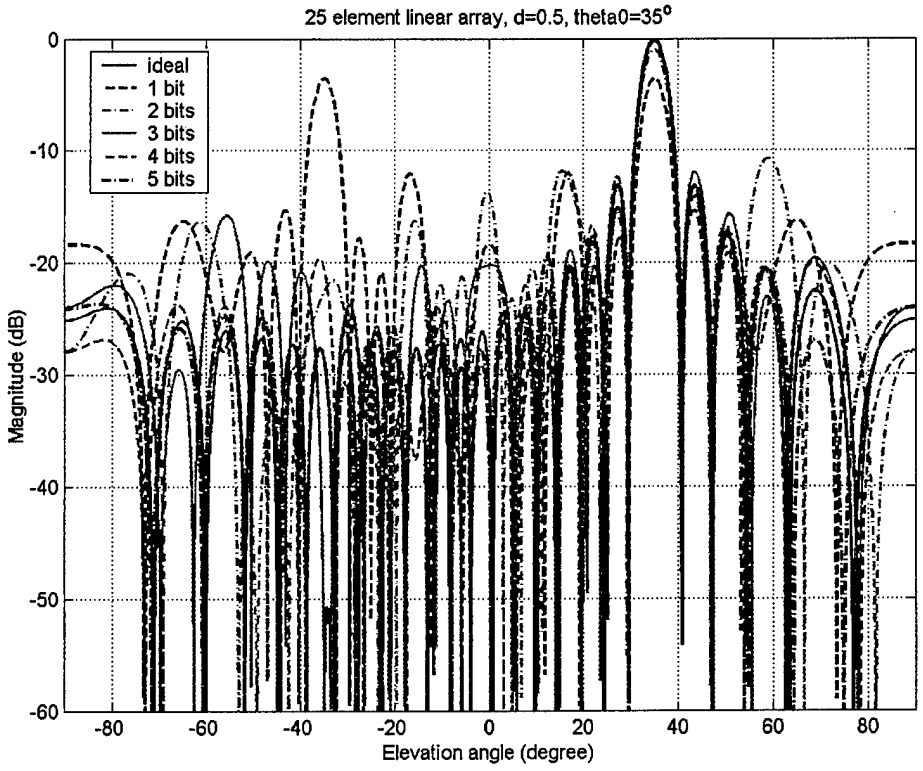

Figure 18: Array factor of a 25-element linear array for a 35°-scan angle

The average results of scan angle deviation, directivity loss and maximum SLL are summarised in *Table 5*.

Table 5 ***Average results of scan angle deviation, maximum SLL and directivity loss over scan angle for 25-element linear array using phase shifters of different numbers of bits***

NUMBER OF BITS OF THE PHASE SHIFTER	1 BIT	2 BITS	3 BITS	4 BITS	5 BITS
Scan angle deviation, $\Delta\theta$ (deg.)	0.46	0.26	0.15	0.066	0.027
$\Delta\theta$ /HPBW (%)	9.37	5.30	2.98	1.26	0.52
Maximum SLL (dB)	-8.13	-9.22	-12.13	-12.67	-12.87
Directivity loss (dB)	3.75	0.85	0.21	0.052	0.013

The average is realised considering a scan angle varying from 0° to 60° with a 1° step

The theoretical maximum SLL is –13.23 dB

3.4 Arrays of 64 elements

The results of a 64 element linear array with a half-wavelength inter-element spacing are presented in this section. The graphs corresponding to an array utilising analogue phase shifters and 2- to 5-bit phase shifters are shown in *Figure 19*.

Figure 19a differs from the previous array factor representation in 2D-colour representation as the horizontal axis is now the elevation angle normalised to the steering angle θ_o, i.e. only the pattern in a 60° beamwidth around the scanning direction is shown. This representation helps to visualise the principal array factor characteristics as the HPBW becomes narrower with the increase of the number of array elements, and as the high side lobes are closer to the main beam. *Figure 19e* shows a similar representation. This is not the case for the other graphs in *Figure 19* because the useful information is not only located arround the main beam.

With 64 elements, the linear array exhibits a 1.6° HPBW in the broadside direction. The HPBW increases slowly to 1.96° for θ_o =35°, and reaches 3.2 for θ_o =60°. Note that the elevation angle step is 0.02° for the array factor computation. The maximum directivity is 21.03 dBi, and the maximum SLL is –13.26 dB.

The array factor of the array with 2-bit phased shifters is depicted in 2D-colour representation in *Figure 19b*. The quantisation lobes appear clearly in this graph. The first QL curve starts at (θ=0°, θ_o =0°), travels in an arc to the (θ=-90°, θ_o =20°) co-ordinate, and then from (θ=90°, θ_o =20°) to (θ=-36°, θ_o =60°). The yellow colour of the curve indicates a –10.5 dB level, as mentioned in *Table 3*. The positions of the QLs are the same as those of the 25-element array with the 2-bit phase shifter. The curves representing the higher QLs are also visible, particularly the second QL with a –14.9 dB level (light blue curves).

The QLs also appear clearly in *Figure 19c*, showing the array factor of the 64-element array with 3-bit phase shifters. In the range $0^o \le \theta_o \le 60^o$, the first QL scans the half space more than three times. The same comment can be made about *Figure 19d*, depicting the array factor

of the 64-element array with 4-bit phase shifters. The curves are thin and dashed and almost invisible, indicating a vanishing effect of the phase quantisation with the increase of the number of the phase shifter bits.

With the 5-bit phase shifters, the QLs are hardly discernible due to the 25 dB colour scale. The representation with the elevation angle normalised to the scan angle for the horizontal axis is then preferred. In the considered scanning range, the difference between the use of analogue phase shifters and 5-bit phase shifters is small. In the later case the QLs are merged with the side lobes, and the combination of the number of array elements and the number of bits gives a number of phase distributions high enough to obtain a scan angle deviation lower than 0.02° over the total considered scanning range.

Figure 19a

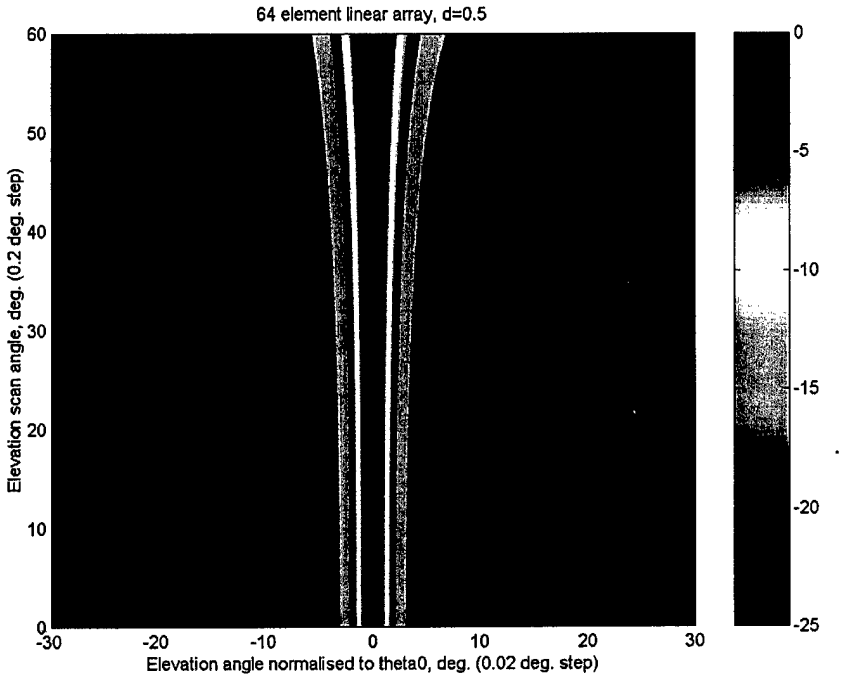

Figure 19b

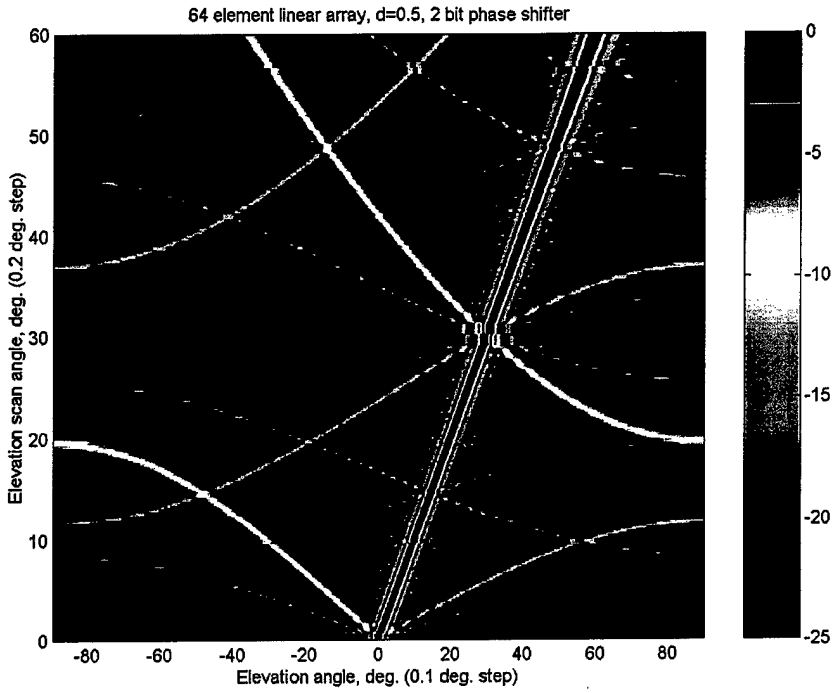

Figure 19c

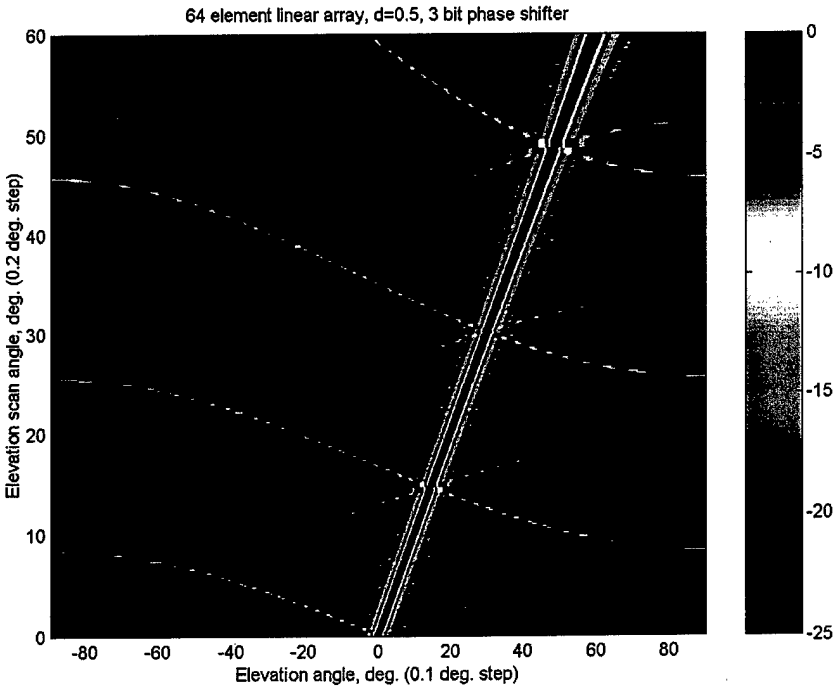

Figure 19d

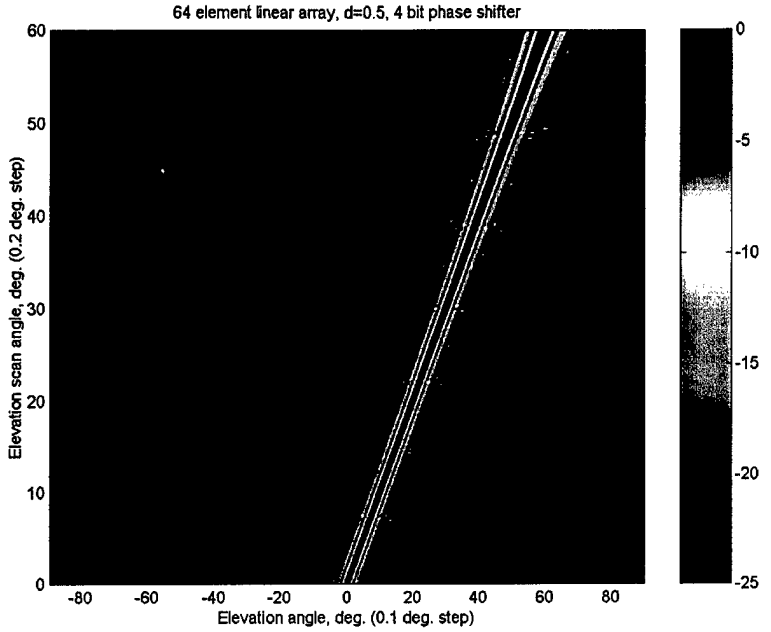

Figure 19e

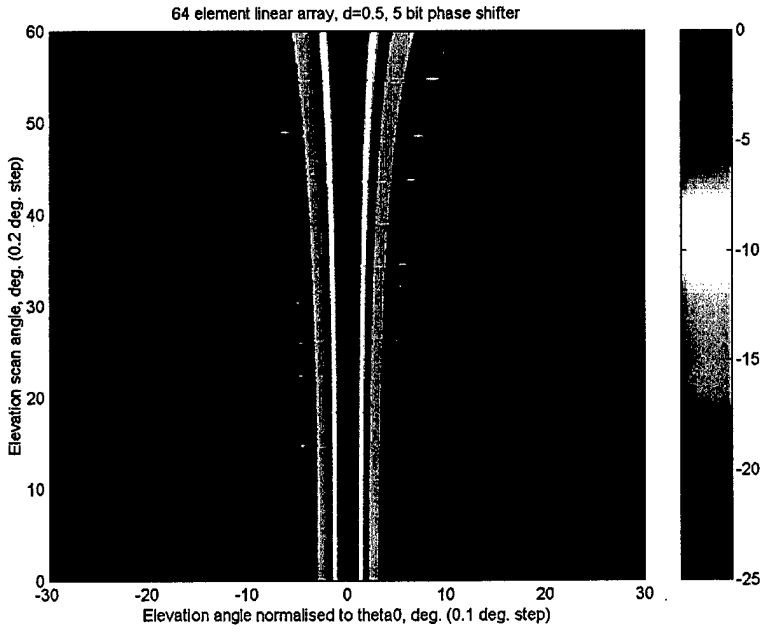

Figure 19: Array factor of a 64-element linear array with a) analogue, b) 2-bit, c) 3-bit, d) 4-bit, e) 5-bit phase shifters (colour scales are in dB)

Table 6 summarises the average results of scan angle deviation, directivity loss and maximum SLL for the 64 element linear array with different phase shifters. As mentioned with the smaller arrays, the overall characteristics are improved with the increase of the number of bits. For this specific array note that the average scan angle deviation normalised to the HPBW equals 1% for 3 bits. The average maximum SLL stays under –12.5 dB from 3 bits as well. The average directivity losses drop below 0.1 dB from 4bits.

Table 6 Average results of scan angle deviation, maximum SLL and directivity loss over scan angle for a 64-element linear array for 2- to 5-bit phase shifters

NUMBER OF BITS OF THE PHASE SHIFTER	2 BITS	3 BITS	4 BITS	5 BITS
Scan angle deviation, $\Delta\theta$ (deg.)	0.064	0.020	0.014	0
$\Delta\theta$ /HPBW (%)	3.28	1.01	0.73	0
Maximum SLL (dB)	-9.18	-12.72	-12.97	-13.13
Directivity loss (dB)	0.90	0.22	0.054	0.013

The average is realised considering a scan angle varying from 0° to 60° with a 1° step

The theoretical maximum SLL is –13.26 dB

The array factor characteristics of three different arrays with digital phase shifters have been detailed and analysed in these sub-sections. They have shown how the characteristics like steering angle, SLL and directivity, are affected by the number of the phase shifter bits. In order to generalise the discrepancy of the array factor characteristics compared to the ideal case versus the number of bits, the results of arrays of other sizes, from 11 to 128 elements are presented thereafter.

3.5 Arrays of other sizes

In this section the array factor characteristics such as steering angle, maximum SLL and directivity losses, of arrays of 11, 32, 45, 85, 110, 115 and 128 elements are presented and summarised. As the variations of the array factors versus the number of bits are similar to those shown previously, only the average results of the parameters mentioned above are reported in *Annex 3*. However, the graphs in *Figure 20* to *Figure 22* summarise the results versus the number of arrays elements with the number of bits as parameter. The cases with arrays of odd and even numbers of elements are separated, as the obtained results differ somewhat.

The scan angle deviation is plotted as a function of the number of elements of the array with the number of the phase shifter bits as a parameter in *Figure 20*. As shown in the previous study, the scan angle deviation decreases with the increase of the number of bits, which causes an increase of the number of possible phase distributions. For a given number of bits, the scan angle deviation also decreases with the increase of the number of elements, also as

the number of possible phase distributions for the array is increasing. Looking at the curves for arrays with odd and even numbers of elements, it appears that their behaviour are linear, i.e., for a same number of bits the curves with odd and even numbers of elements can be merged in a single continuous curve.

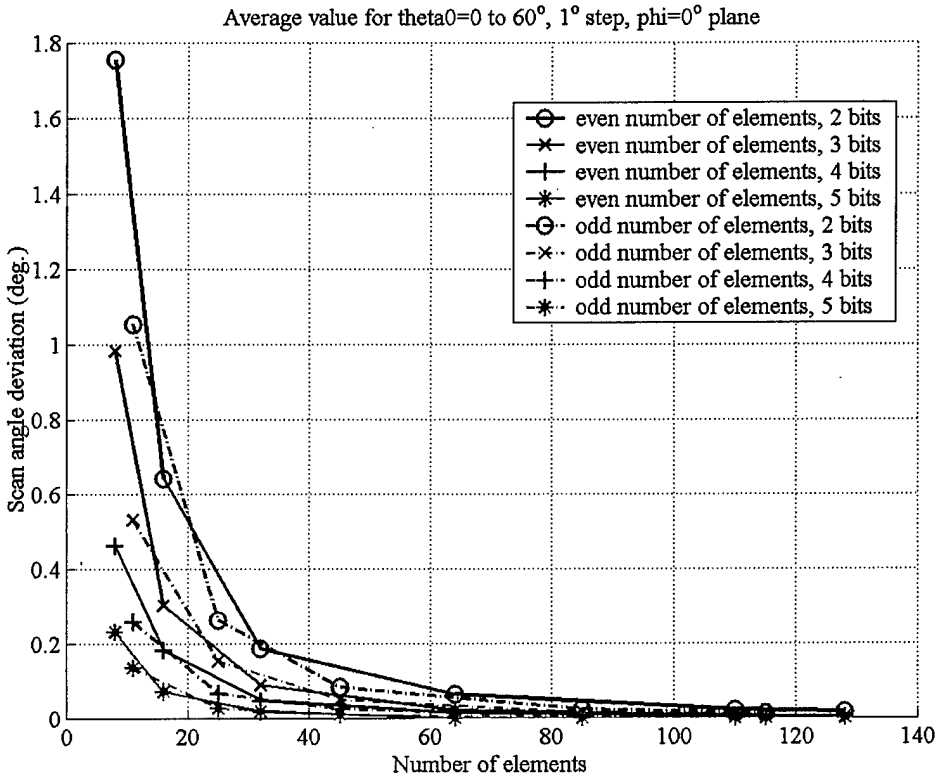

Figure 20: Average Scan angle deviation versus number of array elements

The maximum SLL averaged over the range $0^o \leq \theta_o \leq 60^o$ with a 1° step versus the number of elements is shown in *Figure 21* with the number of bits as parameter. The curves converge toward an absolute value corresponding to the maximum SLL of an infinite array with an analogue phase shifter (-13.26 dB). The slope of the curves depends on the number of bits. For two bits the slope is low and convergence will apparently be achieved for very large arrays. The –12 dB maximum SLL is obtained with only 3 bits from arrays larger than 20 elements, while the –13 dB level is reached with 4 bits for arrays larger than 64 elements, and with 5 bits for arrays as small as 45 elements. For a given number of bits, curves for odd and even number of elements can be merged except for 2 bits. Arrays of odd numbers of elements have lower maximum SLLs over the considered scanning range, but the difference is only about 0.2 dB. However, arrays with a 2-bit phase shifter have an average maximum SLL higher than –10 dB, which is an unacceptable value for most of the applications.

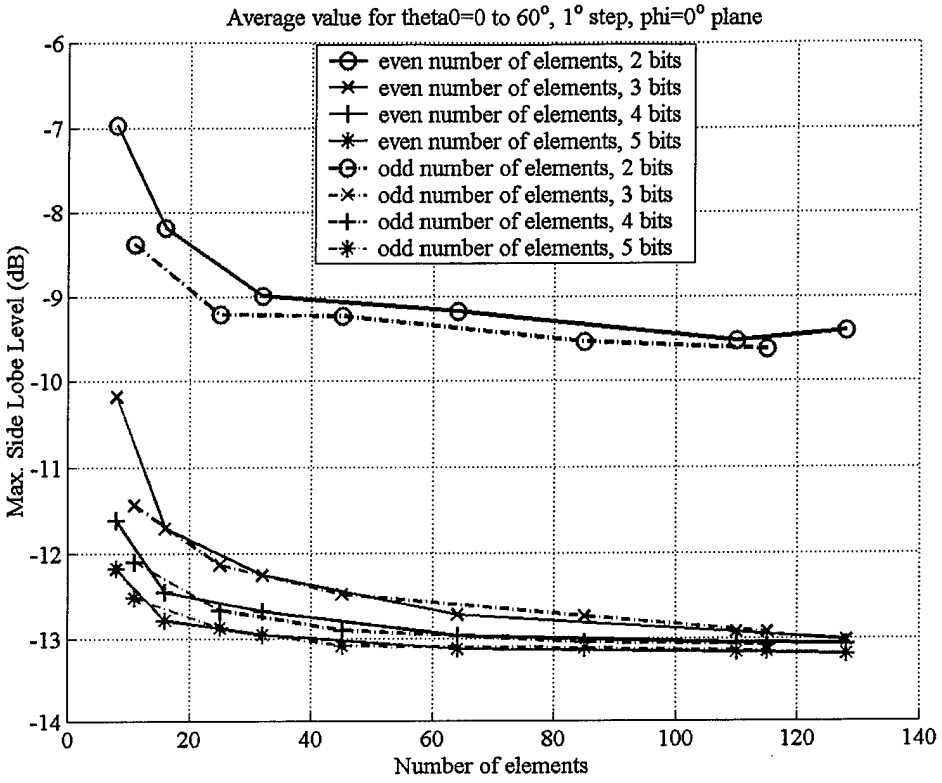

Figure 21: Average maximum SLL versus number of array element)

The difference between arrays of odd and even numbers of elements with a 2-bit phase shifter is reflected on the directivity losses, as shown in Figure 22, even though the difference is only 0.02 dB. As we can see, the directivity loss depends essentially on the number of bits of the phase shifter, even for small arrays. The mean (in terms of array size) directivity losses averaged over a scanning range from $0_o \leq \theta_o \leq 60^o$ with a 1° step are about 0.89 dB, 0.22 dB, 0.0535 dB and 0.013 dB with 2, 3, 4 and 5 bits, respectively. These results are in good agreement with the theoretical ones given in *Table 4*.

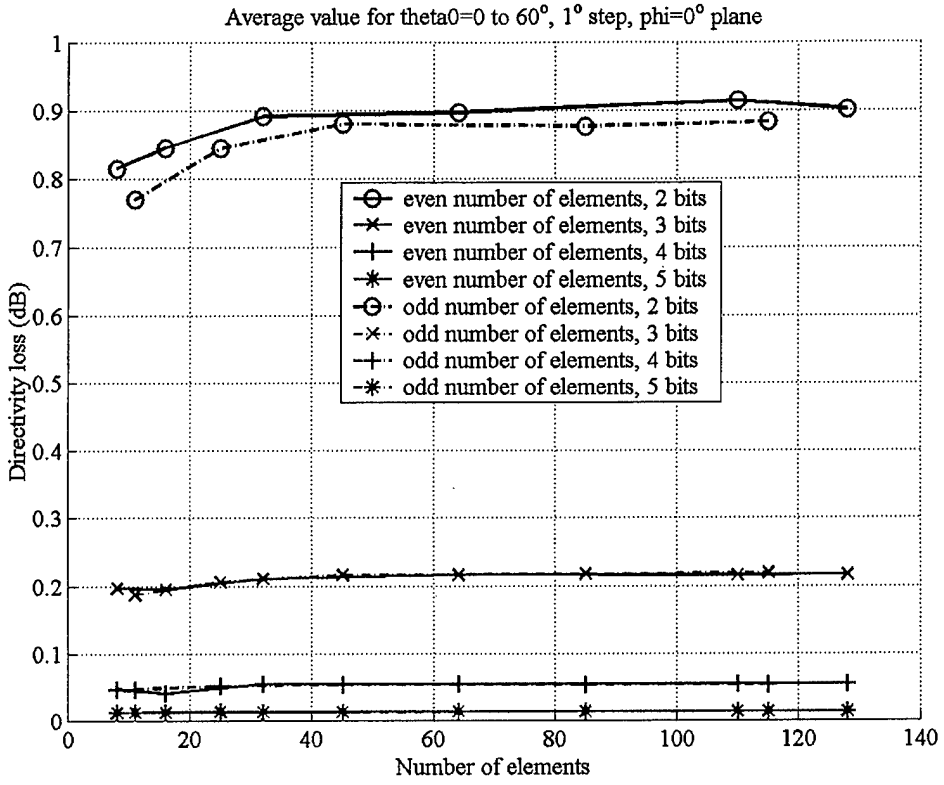

Figure 22: Average directivity loss versus number of array elements

3.6 Concluding remarks

Arrays of different size, in terms of number of elements, with phase shifters with 1 to 5 bits have been studied in this chapter. The effect of the number of bits of the phase shifters on the array factor characteristics has been first pointed out with the investigations on the 8-element phased array. The limited number of phase states for the array, due to quantisation generates a scan angle shift depending on the number of bits and the number of array elements. Increases of the side lobe levels also result, and this introduces directivity losses. The study of the 25-element array showed the generation of side lobes with high levels due to the use of digital phase shifters, called quantisation lobes. Their levels decrease with the increasing number of bits. The results of the 64-element array have confirmed the previous statements qualitatively and quantitatively. And finally, the discrepancy on the array factor characteristics due to the use of digital phase shifters has been quantified for array from 8 to 128 elements. These results are helpful to determine the optimum number of bits considering specific criteria.

For most of the applications, a phase shifter with 3 or 4 bits gives adequate array factor characteristics. For small arrays, the use of 4-bit or even 5-bit phase shifters is preferred because of the reduced number of phase distributions due to the small number of elements, while the use of 3-bit phase shifters is sufficient for arrays larger than 32 elements.

4 The effect of the inter-element spacing

In this section, the effect of the variation of the inter-element spacing on the array factor characteristics is investigated, considering arrays with digital phase shifters. Results of two studies are presented. In the first study, 25-element arrays with different inter-element spacings are considered. In the second study arrays of 12-wavelength length and of different numbers of elements are analysed. Again, the 2D-colour graphs showing the *elevation+scan* plot for each case are used to easily and rapidly visualise the array factor in the main plane versus the scan angle.

In the previous chapter the effect of the number of bits has been studied for arrays with different numbers of elements and with a half-wavelength inter-element spacing. Based on the comments reported in the concluding remarks of that chapter, only the use of the 3-bit phase shifters is considered. As the study is for a single frequency the kind of phase shifter, constant-phased or switched-line, does not matter.

4.1 Arrays of 25 elements with different inter-element spacings

Results for arrays of 25 elements with inter-element spacings of 0.5 to 1.0 wavelength (λ) are presented.

The general characteristics of the different arrays with analogue phase shifters are indicated in *Table 7*. With the increase of the inter-element spacing, the half-power beamwidth decreases regularly, and reaches with the λ-spacing array half the HPBW of the 0.5λ-spacing array. The maximum SLLs remain constant. The maximum directivity, obtained in the broadside direction, becomes larger with the increase of the array size due to the increase of the inter-element spacing. However, the directivity drops for a full wavelength inter-element spacing due to the occurrence of the grating lobe with 0 dB relative magnitude, even when the steering angle corresponds to the broadside direction.

Table 7 ***Characteristics of 25-element arrays of different inter-element spacings, and with analogue phase shifters***

INTER-ELEMENT SPACING (IN WAVELENGTH)	0.5	0.6	0.7	0.8	0.9	1.0
HPBW (deg.)	4.08	3.4	2.92	2.56	2.28	2.04
Maximum SLL (dB)	-13.21	-13.21	-13.21	-13.21	-13.21	-13.21
Maximum directivity (dBi)	16.94	17.72	18.37	18.91	19.33	16.94
Scan angle when grating lobe appears at 90°	90.0	41.81	25.38	14.47	6.37	0.00

Figure 23a

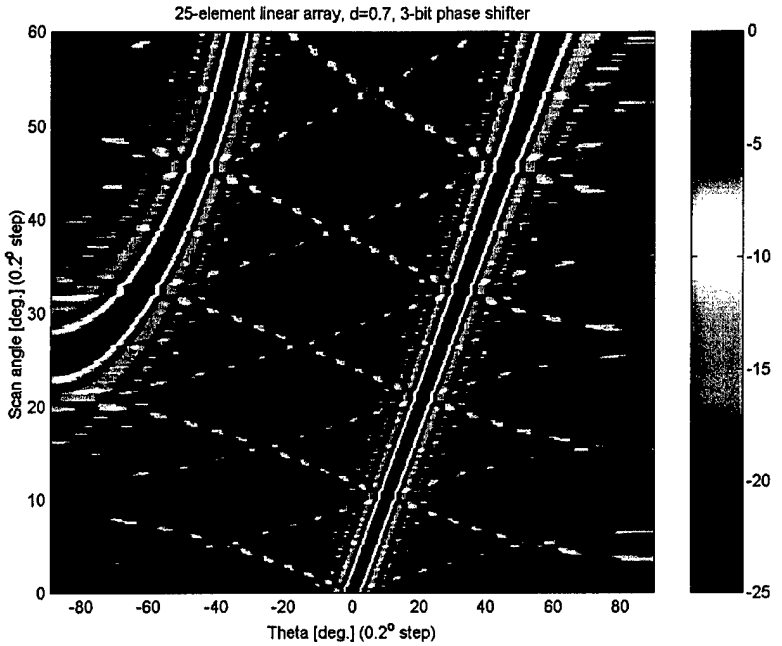

Figure 23b

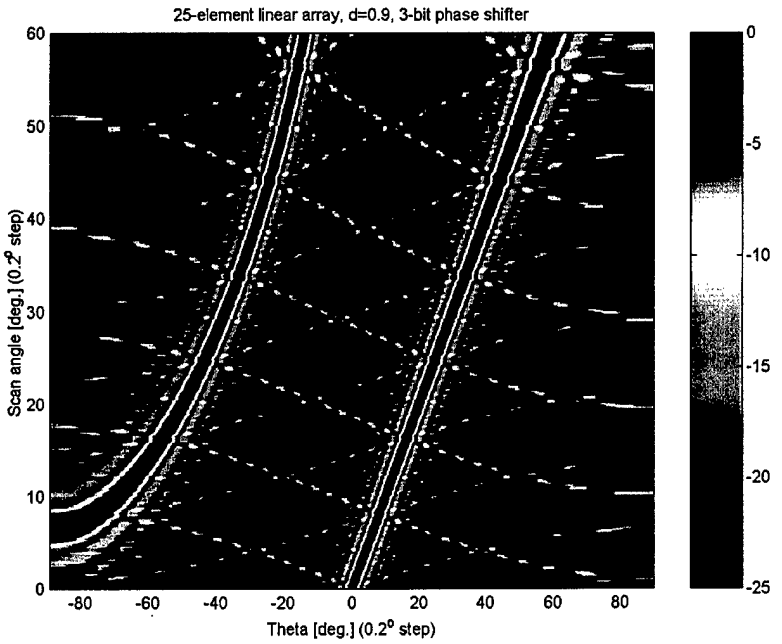

Figure 23: Elevation+scan plots of 25-element arrays with 0.7λ (figure a) and 0.9λ (figure b) inter-element spacings

The graphs representing the *elevation+scan* plot of the array factors with 0.7λ and 0.9λ inter-element spacings are shown in *Figure 23*. The evolution of the grating lobes with theirs side lobes as a function of the scan angle appears clearly in both graphs. For d=0.7λ the grating lobe occurs fully at θ=-90° for θ_0=25.4° while it occurs for θ_0=6.4° with d=0.9λ. The directivity drops significantly for higher scan angles due to the presence of two high level beams, i.e., the main beam and the grating lobe. The quantisation lobes are also well visible with a −17 dB level. When θ_0 increases, the position of the QL varies more rapidly if the inter-element spacing is larger.

The average results over the range $0^o \leq \theta_0 \leq 60^o$ for the 25-element arrays with 0.5 to 1.0 wavelength spacings are reported in *Table 8*. The scan angle deviation normalised to the HPBW is of the same order for all the cases, as well as the average maximum SLL and average directivity loss.

Table 8 ***Average radiation characteristics over scanning range of 25-element arrays of different inter-element spacings with a 3-bit phase shifter***

INTER-ELEMENT SPACING (IN WAVELENGTHS)	0.5	0.6	0.7	0.8	0.9	1.0
Scan angle deviation, Δθ (deg.)	0.15	0.13	0.098	0.074	0.087	0.066
Δθ /HPBW (%)	2.98	2.89	2.63	2.22	3.03	2.50
Maximum SLL (dB)	-12.13	-12.22	-12.22	-12.64	-12.29	-13.21
Directivity loss (dB)	0.20	0.20	0.20	0.19	0.20	0.21

The average is realised considering a scan angle varying from 0° to 60° with a 1° step

Maximum SLL averages have been computed over the scanning range where no grating lobes exist

4.2 Arrays of fixed length with different numbers of elements

For most of the applications, the array antenna must be enclosed in a restricted space. Therefore, the best antenna has to be defined in the available space to meet the specifications. For example, characteristics of arrays of 12λ-length with different numbers of elements are presented in this section. An array of 12λ-length corresponds to a 25-element array with a half-wavelength inter-element spacing. The numbers of elements of the arrays reported here are such that the corresponding inter-element spacings are included in the range [0.5λ;λ].

The main characteristics of the 12λ length arrays are reported in *Table 9*. The half-power beam width slowly decreases with the reduction of the number of elements, as well as the maximum side lobe level averaged over the scanning range where no grating lobes occur. The maximum directivity drops a little bit with the 14-element array while it decreases significantly with the 13-element array due to the progressive appearance of the grating lobe, as the inter-element spacing becomes larger.

Table 9 ***Characteristics of 12-wavelength length arrays of different numbers of elements, with an analogue phase shifter***

NUMBER OF ELEMENTS	25	21	19	17	16	14	13
Element spacing (wavelength)	0.5	0.6	0.667	0.75	0.8	0.923	1.0
HPBW (%)	4.08	4.04	4.04	4.00	4.00	3.96	3.92
Maximum SLL (dB)	-13.21	-13.20	-13.18	-13.16	-13.15	-13.11	-13.09
Maximum directivity(dBi)	16.94	16.96	16.96	16.94	16.92	16.69	14.10
Scan angle when grating lobe appears at -90°	90.0	41.81	29.95	19.47	14.47	4.78	0.0

The *elevation+scan* plots corresponding to a 19-element array and a 16-element array are shown in *Figure 24*. Again, the grating lobes are easily visible in both graphs, appearing at θ=-90° for θ_o=30° with the 19-element array and for θ_o=14.4° with the 16-element array. From this specific steering angle the directivity drops significantly due to the presence of two main beams. The quantisation lobes are well defined on both graphs, forming some green dashed curves in the 2D-colour plot. The comment made in the previous study can be also noticed: when the inter-element spacing becomes larger the positions of the QLs vary more rapidly with increasinge θ_o.

As the number of elements decreases with the increase of inter-element spacing, the number of possible phase distributions decreases. However, the number of possible phase distributions is high enough to avoid a significant increase of the scan angle deviation, as reported in *Table 10*. The variation of the average maximum SLL as a function of the number of elements is not important. In addition, the average directivity loss over the range $0^o \leq \theta_o \leq 60^o$ remains constant when the number of elements is reduced.

Table 10 ***Average radiation characteristics over scanning range for the 12λ length arrays of different numbers of elements, with 3-bit phase shifters***

NUMBER OF ELEMENTS	25	21	19	17	16	14	13
Element spacing (wavelength)	0.5	0.6	0.667	0.75	0.8	0.923	1
Scan angle deviation, Δθ (deg.)	0.15	0.17	0.15	0.15	0.20	0.20	0.21
Δθ /HPBW (%)	2.98	3.53	2.91	3.11	4.16	4.02	4.17
Maximum SLL (dB)	-12.13	-12.15	-11.78	-12.01	-11.57	-11.96	-13.09
Directivity loss (dB)	0.21	0.20	0.21	0.19	0.20	0.20	0.19

The average is realised considering a scan angle varying from 0° to 60° with a 1° step

Maximum SLL averages have been computed over the scanning range where no grating lobes exist

Figure 24a

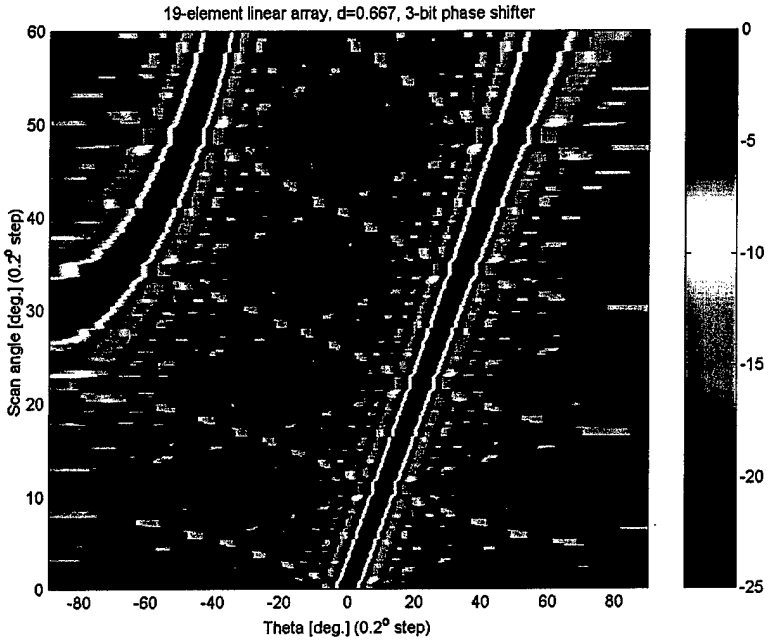

Figure 24b

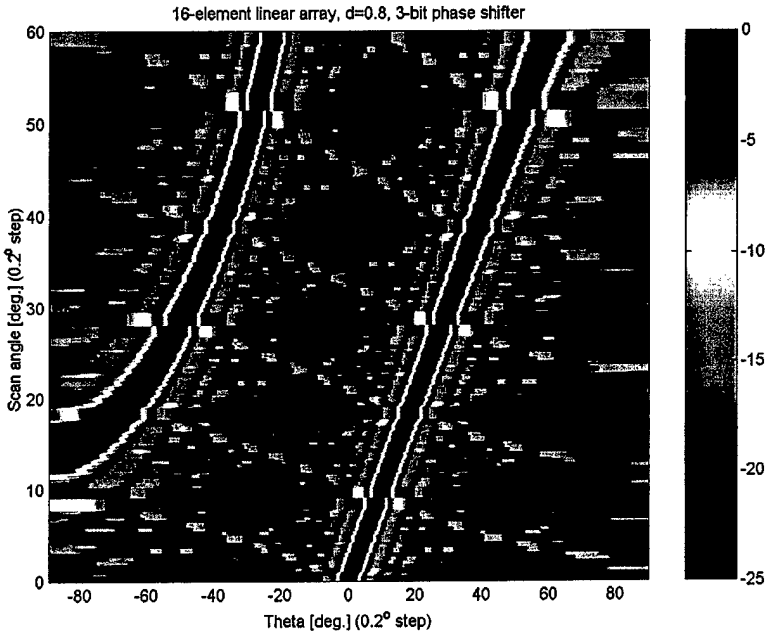

Figure 24: Elevation+scan plot of arrays of 12λ length: a) 19-element array with 0.667λ inter-element spacing, b) 16 element array with 0.8λ inter-element spacing

4.3 Concluding remarks

The effect of the inter-element spacing has been clearly identified with the help of the 2D-colour representation of the *elevation+scan* plot. The occurrence of the grating lobes is well and quickly visible as a function of the scan angle, as well as the appearance of the quantisation lobes.

The first study, where the spacing of a constant number of array elements is the parameter, shows that the average radiation characteristics do not vary significantly, considering digital phase shifters.

The second study, where the total length of the array is kept constant and the inter-element spacing is varied by decreasing the number of elements, shows that the scan angle discrepancy slightly increases with the increase of the inter-element spacing. This is due to a smaller number of possible phase distributions across the array, because of the reduction of the number of elements. The other average characteristics, i.e., the maximum side lobe level and the directivity loss, remain unchanged.

5 Array characteristics versus frequency

In this chapter, the variations of the array factor with frequency are investigated. For this study a 25-element array with a half-wavelength inter-element spacing is considered. Results of arrays with constant-phase phase shifters (analogue and digital with 3-bits) and switched-line phase shifters (analogue and digital with 3 bits) are compared to those of an array with true-time-delay lines. The phase weighting applied to each element is defined at 30 GHz. The frequency range of interest is 1 to 50 GHz.

5.1 Arrays with true-time-delay feed network

This section presents the array factor of a 25-element array with a half-wavelength inter-element spacing with feed networks having true-time-delay lines. The results of the AFs are shown with 2D-colour plots for easier and faster analysis. Mathematical equations describing the main features in the graphs are also developed.

Before introducing the results for a 35° scan angle, the *elevation+frequency* plot of the array factor of a 25-element array with a true-time-delay lines pointing in the broadside direction is depicted in 2D-colour polar plot in *Figure 25*. Although the plot is in the polar co-ordinate system, the colour curves representing the main lobe (red curve) and the side lobes (light blue and green curves) are straight lines. This indicates that the overall characteristics (lobe and null positions, HPBW) are varying as a function of the inverse of the frequency.

Indeed, as the lengths of the delay lines are the same for each element, the particular array factor corresponds to the one of an array with uniform phase and amplitude distributions. Therefore, the AF is expressed by

$$AF(\theta) = \frac{\sin\left[N\pi\frac{d}{\lambda}\sin(\theta)\right]}{N\sin\left[\pi\frac{d}{\lambda}\sin(\theta)\right]} \qquad \textit{(eq. 11)}$$

where

- N is the number of array elements,
- d is the inter-element spacing,
- λ is the wavelength,
- θ is the elevation angle as defined in *Figure 5*, page 7.

The positions of the minima and grating lobes, for instance, are given by *(eq. 12)* which is the equation of a straight line in the polar co-ordinate system (see *Annex 4*) [8].

$$\textit{(eq. 12)} \qquad N\pi\frac{d}{\lambda}\sin(\theta_p) = p\pi, \qquad \text{or}$$

$$\textit{(eq. 13)} \qquad \sin(\theta_p) = \frac{p}{Nd}\frac{c}{f}$$

where

- p is an integer,
- c is the speed of the light,
- f is the frequency,
- θ_p is the pth minima or grating lobes.

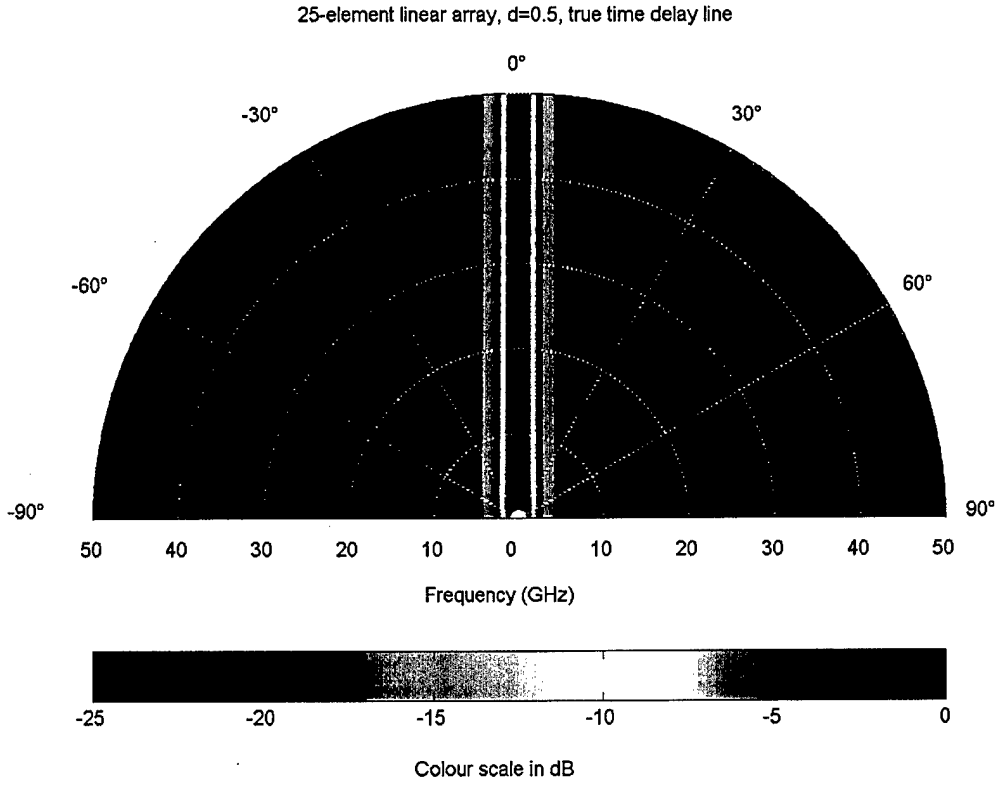

Figure 25: 2D-colour polar plot of the array factor versus frequency of a 25-element linear array, with a feed system using true-time-delay lines, pointing in the broadside direction

With the same array configuration, the array factor with a scan angle θ_o is expressed by

$$\textit{(eq. 14)} \qquad AF(\theta) = \frac{\sin\left\{N\pi\frac{d}{\lambda}\left[\sin(\theta)-\sin(\theta_o)\right]\right\}}{N\sin\left\{\pi\frac{d}{\lambda}\left[\sin(\theta)-\sin(\theta_o)\right]\right\}}$$

The scan angle is given by *(eq. 2)* page 5, with n=1. This equation reduces to $L_o = d\sin(\theta_o)$, and L_o represents the length of the elementary true-time-delay line.

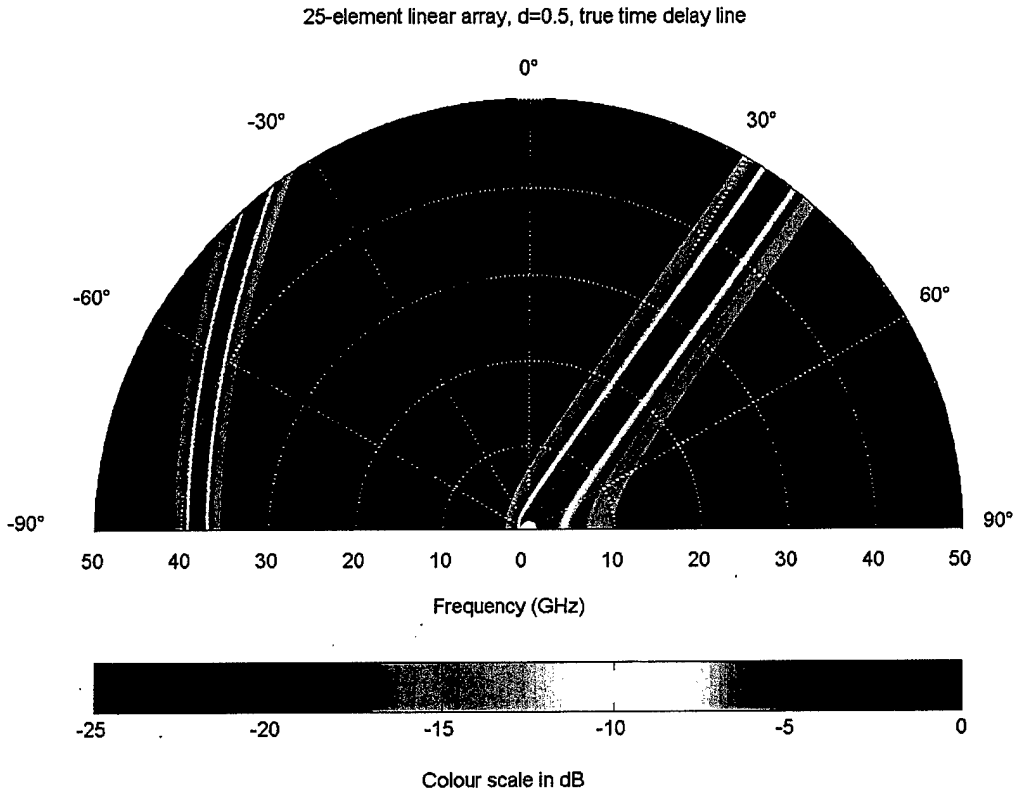

Figure 26: 2D-colour polar plot of the array factor versus frequency of a 25-element linear array, with a feed system using true-time-delay lines, pointing in the θ_o=35° direction

Considering a scan angle of θ_o, the positions of the minima and grating lobes are given by

$$\textit{(eq. 15)} \qquad N\pi\frac{d}{\lambda}\left[\sin(\theta_p)-\sin(\theta_o)\right] = p\pi \qquad \text{or}$$

(eq. 16)
$$f = \frac{p}{Nd\sin(\theta_o)} \frac{c}{\frac{\sin(\theta_p)}{\sin(\theta_o)} - 1}$$

As $1/\sin(\theta_o)>1$, the equation corresponds to that of a hyperbola (see *Annex 4*)[8]. This is illustrated in *Figure 26* where the array factor of a 25-element array with true-time-delay lines, pointing in the 35° direction, is plotted in the *elevation+frequency* graph.

The grating lobe (GL) appears clearly on the left side of the plot, for frequencies above 38 GHz. The GL occurs when

(eq. 17)
$$\frac{d}{\lambda} = \frac{1}{\left[\sin(\theta_p) - \sin(\theta_o)\right]}$$

where θ_g is the position the grating lobe maximum.

In the considered case, the inter-element spacing is a half-wavelength at f_o=30 GHz and the scanning angle θ_o is 35°. The above equation becomes

(eq. 18)
$$f = \frac{2f_o}{\sin(\theta_o)} \frac{1}{1 - \frac{\sin(\theta_g)}{\sin(\theta_o)}}$$

The first grating lobes occurs at –90° for 38.1 GHz and at –38.8° for 50 GHz. Note that *(eq. 18)* corresponds to the equation of a hyperbola.

5.2 Arrays with constant-phase phase shifters

A 25-element array with a half-wavelength spacing with constant phase shifters is now investigated. We consider first an analogue constant-phase phase shifter, i.e., the phase weighting the n^{th} antenna element at the frequency f_o is exactly the required phase to steer in the θ_o direction, or

(eq. 19)
$$\varphi_n = n\,\varphi_o \qquad \text{with} \qquad \varphi_o = \frac{2\pi}{\lambda_o} d\sin(\theta_o)$$

where λ_o is the wavelength at f_o.

The array factor is then expressed with

$$\textit{(eq. 20)} \qquad AF(\theta) = \frac{\sin\left\{N\pi\frac{d}{\lambda}\left[\sin(\theta) - \frac{\varphi_o}{2}\right]\right\}}{N\sin\left\{\pi\frac{d}{\lambda}\left[\sin(\theta) - \frac{\varphi_o}{2}\right]\right\}}$$

The positions of the minima and grating lobes are given by

$$\textit{(eq. 21)} \qquad N\pi\frac{d}{\lambda}\left[\sin(\theta_p) - \frac{\varphi_o}{2}\right] = p\pi \qquad \text{or}$$

$$\textit{(eq. 22)} \qquad \sin(\theta_p) = \frac{\left(p\pi + \frac{\varphi_o}{2}\right)}{N\pi d}\,\frac{c}{f}$$

This expression is the equation of a straight line in the polar co-ordinate system (see *Annex 4*), and can be seen in the corresponding *elevation+frequency* plot depicted in *Figure 27*.

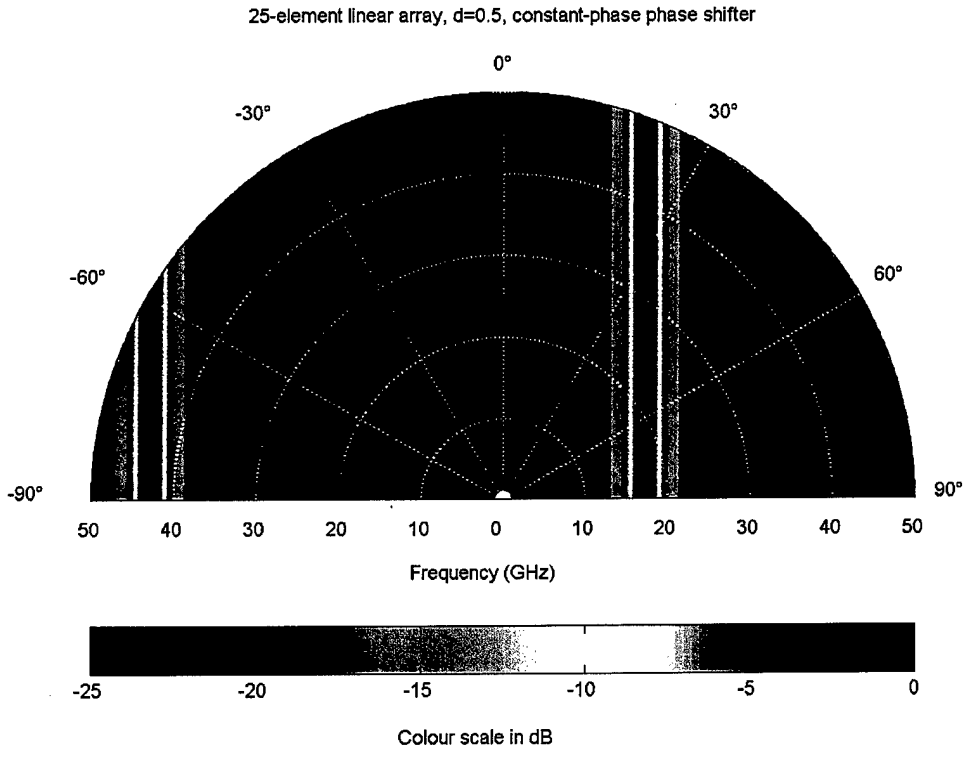

Figure 27: 2D-colour polar plot of the array factor versus frequency of a 25-element linear array, with analogue constant-phase phase shifters, pointing in the direction θ_o=35° at f_o=30GHz

Figure 27 also shows the grating lobe, which occurs at 42 GHz and above. The frequency where the GL appears can be determined using *(eq. 17)*, where θ_o is now varying with frequency. The expression of the scan angle versus frequency, $\theta_o(f)$, is

$$\textit{(eq. 23)} \qquad \sin[\theta_o(f)] = \frac{f}{f_o}\sin[\theta_o(f_o)]$$

The above equation is simply obtained by equating the denominator of the array factor given in *(eq. 20)* to zero, which also determines the position of the AF maximum.

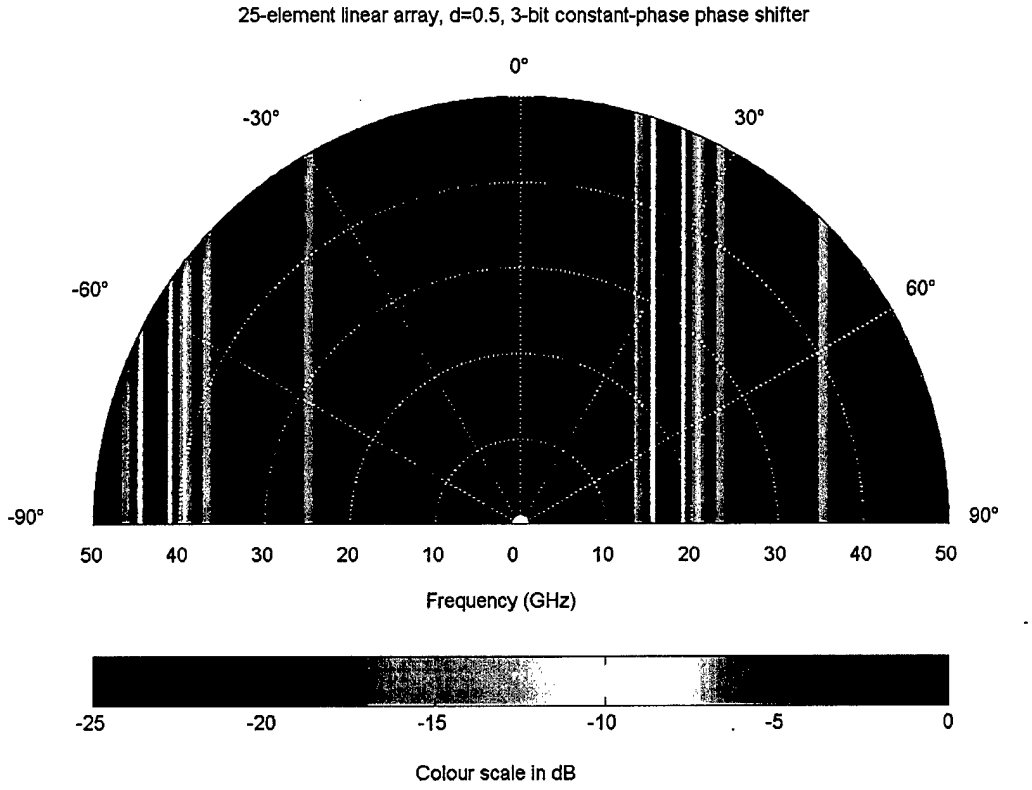

Figure 28: 2D-colour polar plot of the array factor versus frequency of a 25-element linear array, with 3-bit digital constant-phase phase shifters, pointing in the direction θ_o=35° at f_o=30GHz

The *elevation+frequency* plot of a 25-element array with a half-wavelength inter-element spacing fed through 3-bit constant-phase phase shifters is presented in *Figure 28*. The graph is similar to the previous one. Because the phase shifter is digital, quantisation lobes occur, and their variation versus frequency implies additional straight lines. Note also that for this array and this configuration, the side lobe levels on each side of the main beam are not symmetric and the ones on the right side have higher magnitude.

5.3 Arrays with switched-line phase shifters

The *elevation+frequency* plot of a 25-element array with a half-wavelength inter-element spacing with a 3-bit switched-line phase shifter is presented in *Figure 29*. This figure shows first that array factors with only one lobe with high level (0 dB or so) appear in a small frequency range around f_o (f_o=30 GHz is the considered frequency for the calculation of the switched-line lengths), called hereafter the clear zone of the frequency range.

The variations of the high-level lobe positions versus frequency are straight lines whose level is fluctuating. Particularly, a high level lobe occurs in the broadside direction. The magnitude is 0 dB at low frequency and decreases until the lobe vanishes below –25dB throughout the clear zone of the frequency range. Finally this lobe appears again with a significant level at higher frequency.

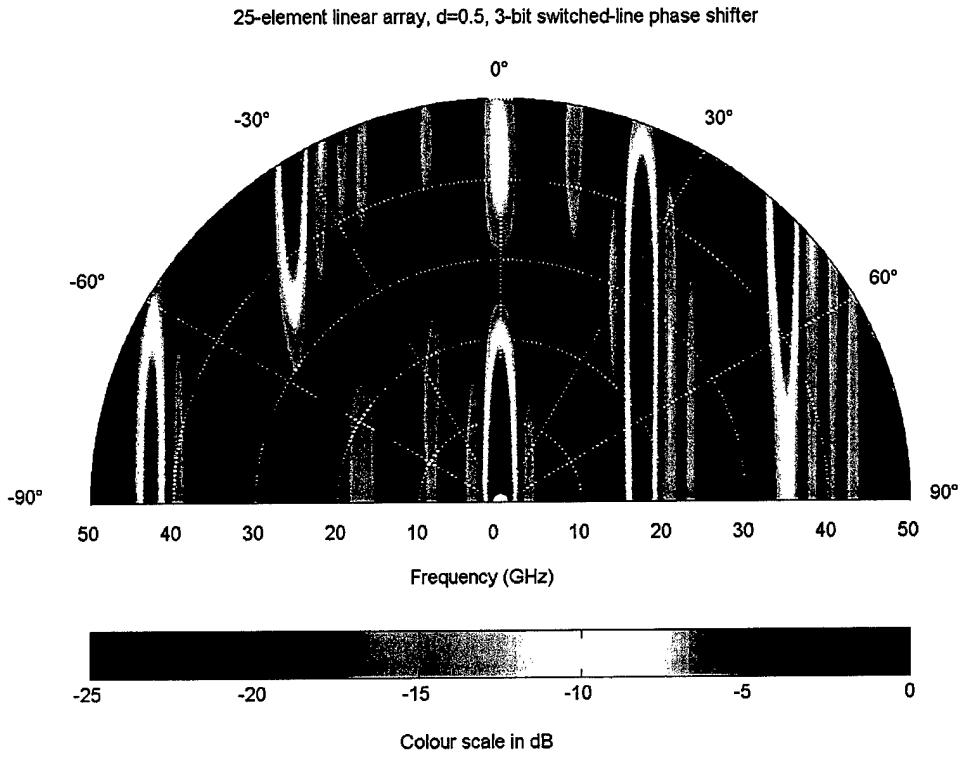

Figure 29: 2D-colour polar plot of the array factor versus frequency of a 25-element linear array with 3-bit switched-line phase shifters, pointing in the direction θ_o=35° at f_o=30GHz

For comparison purposes, the *elevation+frequency* plot of the array factor of the same 25-element array, but with analogue switched-line phase shifters, is shown in *Figure 30*. By

definition, an analogue switched-line phase shifter consists of switched-lines whose length gives the required phase to steer the beam in the desired direction θ_o at a specific frequency f_o.

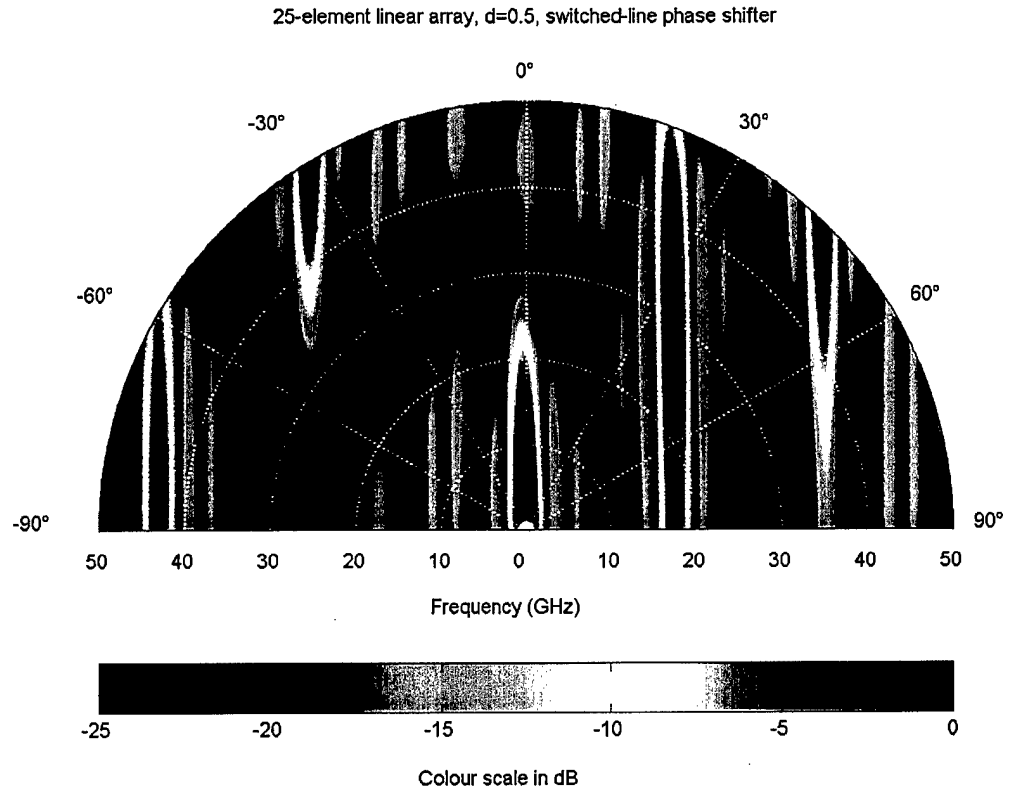

Figure 30: 2D-colour polar plot of the array factor versus frequency of a 25-element linear array with analogue switched-line phase shifters, pointing in the direction θ_o=35° at f_o=30GHz

5.4 Concluding remarks

The frequency dependence of the array factor has been investigated considering a 25-element linear array with a half-wavelength inter-element spacing fed through true-time-delay lines, constant-phase phase shifters and finally switched-line phase shifters. Using the 2D-colour plot the side lobes, grating lobes and quantisation lobes have been clearly identified and mathematically described.

The use of true-time-delay lines in the feed network gives the best results, keeping the scan angle constant over the frequency range. The use of both phase shifters introduces a frequency dependence on the scan angle, which is clearly visible in straight colour lines in the 2D-colour polar plots. The constant-phase phase shifter is preferred as no 0 dB magnitude lobes other than grating lobes are added. However, the switched-line phase shifter is the more realistic one, and gives the worst results on a broadband utilisation.

6 Conclusion

This document has presented the results of investigations on radiation characteristics of linear arrays using feed networks with digital phase shifters. Arrays of point source elements, having different sizes in terms of number of elements and inter-element spacings, have been considered. Studies of array factor characteristics have been carried out over specified scanning and frequency ranges.

In the first part the impact of changes in the number of digital phase shifter bits on the radiation characteristics have been pointed out by detailed studies of arrays of various numbers of elements. With the help of two-dimensional colour graphic representations it has been shown qualitatively that the limited number of phase distributions across the array, due to quantisation:

- generates scan angle discrepancies depending on the number of bits and the number of array elements,
- increases side lobe levels,
- introduces additional lobes called quantisation lobes, whose levels depend on the number of bits,
- and as a result of all the above, decreases the directivity.

All these characteristics have been quantified for arrays of different sizes, with phase shifters of different numbers of bits. This has helped to determine the optimum number of bits considering a specific criterion.

Thus, for most applications and considering the overall characteristics, 3-bit digital phase shifters are sufficient for large arrays. The 4-bit and even 5-bit digital phase shifters are preferred for small arrays because of the reduced number of possible phase distributions due to the small number of elements.

A second study has been carried out considering the inter-element spacing as a parameter, and with digital phase shifters of different numbers of bits. The first part has presented the results of 25-element arrays with various inter-element spacings. It has been shown that the average radiation characteristics do not vary with changes in this parameter, for digital phase shifters with a given number of bits. The second part was about the characteristics of 12-wavelength length arrays with different inter-element spacings, and thus, different numbers of elements. It has been shown that the scan angle deviation is slightly increased with the increase of the spacing between elements. This is due to a smaller number of possible phase distributions, because of the reduction of the number of elements.

In the last chapter, the characteristics of 25-element arrays have been investigated as a function of frequency, when true-time-delay lines, constant-phase and switched-line phase shifters (analogue or digital) were considered. The different effects of frequency on the array factor have been clearly identified with the help of the two-dimensional colour graphic representations, and mathematical descriptions have been provided. Best results have been achieved with true-time-delay lines, which maintain the scan angle constant over the frequency range. The two kinds of phase shifters, constant-phase and switched-line phase shifters, bring a frequency dependence on the scan angle. The latter, which is the most realistic, generates additional high-level lobes, so is the worst phase shifter for utilisation over a broad frequency range.

These results have been provided with the computer program, which is described in the second chapter. This first version allows the study of different kinds of arrays considering theoretical analogue and digital phase shifters. Models of realistic phase shifters will be implemented in the future. In addition, mutual coupling between radiating elements, which is an important parameter in phased array studies, should be considered, as well as the radiation patterns of different elements. Computations taking into account such features would provide results closer to measured characteristics, and can be compared to the results reported in this document.

References

[1] Antenna Theory: analysis and design, C.A. Balanis, John Wiley and sons, 2nd Edition, 1997.

[2] Phased array antenna handbook, R.J. Mailloux, Artech House, 1994.

[3] Phased array antennas, R.C. Hansen, John Wiley and sons, 1998.

[4] Minimizing the effects of phase quantization errors in an electronically scanned array, C.J. Miller, Proc. 1964 Symp. Electronically Scanned Phased Arrays and Applications, RADC-TDR-64-225, Griffiss AFB, Vol.1, pp 17-38.

[5] The handbook of antenna design, A.W. Rudge, K. Milne, A.D. Olver, P. Knight, published by Peter Peregrinus Ltd, 1986.

[6] Phased array radar studies, J. L. Allen and al, Lincoln Lab MIT. TR 238, August 1960.

[7] Array grating lobes due to periodic phase, amplitude and time-delay quantization, R.J. Mailloux, IEEE Trans, on Antennas and Propagation, Vol. AP-32, No12, December 1964, pp 1364-1368.

[8] The VNR concise encyclopedia of mathematics, W. Gellert, H. Küster, M. Hellwich and H. Kästner, Van Nostran Reinhold Company, N.Y., 1977.

Annexes

Annex 1 Description of the input file data

The input file contains the information needed for computation and visualisation processes. The file can also contain some comments. Each input data follows text describing its nature. This text must occur before the data. If not, the data is not read properly by the software.

A reference input file, called *paasom_input_data_hlp.txt*, contains all the possible variables with their different possible values. It allows the user to create a separate file using the "cut and paste" function. The following table details all the input data and the values they can take.

	Data name	Data value	Comment
Array Characteristics	Array geometry (ar_geo)	Linear Rectangular Triangular Circular Hexagonal Octagonal other	If other, the user has to create a file containing the Cartesian co-ordinates of the elements
	Array lattice (ar_lattice)	Rectangular Triangular Hexagonal other	If other, the user has to create a file containing the Cartesian co-ordinates of the elements Array lattice is not required for circular or other geometry
	Number of element (*nb_elt*)	nb_elt[1] (nbx,nby)[2] (nbr, nbp_1: nbp_2:...: nbp_{nbr})[3]	[1] : case linear [2] : maximum number of element along horizontal and vertical axis [3] : case circular; nbr is the number of rings, nbp_is are the number of elements for each ring
	Inter-element spacing* (*spacing*)	Spacing[1] (dx1:dx2:...:dx3,dy)[2] (rd_1:rd_2:...:rd_{nbr},dp)[3]	* in wavelengths @ Fo [1] : case linear [2] : maximum number of elements along horizontal and vertical axes [3] : case circular; rd_i is the spacing between the ith and ith-1 rings, dp is the inter-element spacing between elements on a same ring
	angle of the first element of each ring* (*phase_deb*)	(fp1,fp2,...,fp_{nbr})	* for circular geometry
	Max. number of element per subarray (*nb_elt_sub*)	nb_elt_sub (nb_elt_sub_x,nb_elt_sub_y)	Maximum number of elements in the sub-array along horizontal and vertical axes
	element radiation pattern (*elt_rad_filename*)	filename.erp	Filename which contains element radiation pattern

	Data name	Data value	Comment
Frequency (GHz)	center frequency (Fo)	Fo	Frequency used for phase computation
	frequency range *(freq)*	Fstart:Fstep:Fstop F1 :F2 :... :Fn	
Phase shifter Characteristics	type of phase shifter (phase_shifter_type)	constant phase constant delay	
	number of bits *(nb_bit)*	nb_bit (nb_bit_{start}:nb_bit_{stop}) (nb_bit_1:nb_bit_2:...:nb_bit_n)	
Amplitude Characteristics	amplitude distribution (ampl_distr)	Uniform Cosine Chebyshev	
	amplitude parameter *(ampl_par)*	(ap_1,ap_2,...,ap_N)	
Spatial Data	scanning direction *(theta0, phi0)*	(θ_0,φ_0) (θ_{0start}:θ_{0step}:θ_{0stop},φ_0) (θ_{0start}:θ_{0step}:θ_{0stop},φ_{0start}:φ_{0step}:φ_{0stop}) (θ_0,φ_{0start}:φ_{0step}:φ_{0stop})	
	visualisation space *(theta, phi)*	(θ,φ) (θ_{start}:θ_{step}:θ_{stop},φ) (θ_{start}:θ_{step}:θ_{stop},φ_{start}:φ_{step}:φ_{stop}) (θ,φ_{start}:φ_{step}:φ_{stop})	
Results	first parameter (res_par)	Theta0 Phi0 Theta0phi0[1] freq nb_bit	[1] : Theta0 and phi0 are varying together. If they are vectors, they must have the same dimensions
	Result *(res(1))*	array factor radiation pattern	Res(1)=1 if array factor selected
	optional result *(res(2),res(3),res(4))*	maximum directivity lobe characteristics element radiation pattern	Res(i)=1 if the corresponding option is selected
Visualisation	type of visualisation (vizu)	2D 2Dcolor	Visu(1)=1 if 2D selected Visu(2)=1 if 2Dcolor selected
	Visualisation parameter Vizu_par1	Theta Phi Theta_norm[1] Phi_norm[2]	[1] : Theta normalised to theta0 [2] : Phi normalised to phi0
	Visualisation parameter Vizu_par2	Theta Phi Theta0 Phi0 Theta0phi0[1] freq nb_bit	[1] : Theta0 and phi0 are varying together. If they are vectors, they must have same dimensions
	coordinate system (coord_sys)	cartesian Polar	

Annex 2 Description of PAASoM main functions

The following table indicates the input and output data of the main functions. Some of them use secondary functions not mentioned in this report. The data shown in this table are scalar, vector or table. The vectors are indicated in *italic style* and the tables in *underline italic style*.

Function Name	Input data	Output data	Comment
AFcalculation	*Postab* *Amplvec* *Phasvec* *theta* *phi*	*AF*	- Compute the array factor for (theta,phi)
creer_postab	filename ar_geo ar_lattice *nb_elt_u, nb_elt_v* *spacing_u, spacing_v* *phas_deb* Fo	*Postab*	- Compute the Cartesian co-ordinates of each element (x,y,z), considering the array geometry and lattice
creer_phasvec	Filename *Postab* Fo phase_shifter_type *nb_bit* *theta0* *phi0*	*Phasevec*	- Determine the phase of each element taking into account the kind of phase shifter
creer_amplvec	Filename *Postab* Ar_geo ampl_distr ampl_par *nb_elt_u, nb_elt_v*	*Amplvec*	- Determine the amplitude of each element considering specific distribution law
visualisation	visu coord_syst *res_par* vizu_par1 visu_par2 visu_par3 *AR*	none	- Visualise results - visu_par3 will be considered later for multiple windows visualisation
calcul_maxdir	*postab* *amplvec* *phasvec* *freq*	max_dir	- Compute the maximum directivity
find_lobechar	*AR* *theta* *phi*	*lobechar*	- Find the lobe characteristics of the AR (i.e. location, level, HPBW)

Function Name	Input data	Output data	Comment
read_erp	filename.erp (elt_rad_filename)	*Erptab* *theta* *phi*	- Read file containing radiation pattern data

Annex 3 Tables of average results of scan angle deviation, maximum SLL and directivity loss over scan angle for arrays of different numbers of elements, fed through phase shifters of different numbers of bits

The average is realised considering a scan angle varying from 0° to 60° with a 1° step.

Table 11 ***Averages of scan angle deviation, maximum SLL and directivity loss over scan angle for 11-element linear array with 2- to 5-bit phase shifter***

NUMBER OF PHASE SHIFTER BITS	2 BITS	3 BITS	4 BITS	5 BITS
Scan angle deviation, $\Delta\theta$ (deg.)	1.06	0.53	0.26	0.13
$\Delta\theta$ /HPBW (%)	9.02	4.55	2.13	1.14
Maximum SLL (dB)	-8.38	-11.45	-12.09	-12.52
Directivity loss (dB)	0.77	0.19	0.047	0.012

The theoretical maximum SLL is –13.02 dB

Table 12 ***Averages of scan angle deviation, maximum SLL and directivity loss over scan angle for 16-element linear array with 2- to 5-bit phase shifter***

NUMBER OF PHASE SHIFTER BITS	2 BITS	3 BITS	4 BITS	5 BITS
Scan angle deviation, $\Delta\theta$ (deg.)	0.64	0.30	0.18	0.07
$\Delta\theta$ /HPBW (%)	8.14	3.65	2.33	0.88
Maximum SLL (dB)	-8.19	-11.71	-12.45	-12.78
Directivity loss (dB)	0.85	0.19	0.041	0.012

The theoretical maximum SLL is –13.15 dB

Table 13 ***Averages of scan angle deviation, maximum SLL and directivity loss over scan angle for 32-element linear array with 2- to 5-bit phase shifter***

NUMBER OF PHASE SHIFTER BITS	2 BITS	3 BITS	4 BITS	5 BITS
Scan angle deviation, $\Delta\theta$ (deg.)	0.186	0.089	0.048	0.018
$\Delta\theta$ /HPBW (%)	4.78	2.16	1.26	0.46
Maximum SLL (dB)	-8.99	-12.25	-12.68	-12.96
Directivity loss (dB)	0.89	0.21	0.054	0.013

The theoretical maximum SLL is –13.23 dB

Table 14 ***Averages of scan angle deviation, maximum SLL and directivity loss over scan angle for 45-element linear array with 2- to 5-bit phase shifter***

NUMBER OF PHASE SHIFTER BITS	2 BITS	3 BITS	4 BITS	5 BITS
Scan angle deviation, $\Delta\theta$ (deg.)	0.084	0.048	0.024	0.010
$\Delta\theta$ /HPBW (%)	2.92	1.69	0.86	0.35
Maximum SLL (dB)	-9.23	-12.48	-12.91	-13.09
Directivity loss (dB)	0.88	0.22	0.054	0.013

The theoretical maximum SLL is –13.25 dB

Table 15 ***Averages of scan angle deviation, maximum SLL and directivity loss over scan angle for 85-element linear array with 2- to 5-bit phase shifter***

NUMBER OF PHASE SHIFTER BITS	2 BITS	3 BITS	4 BITS	5 BITS
Scan angle deviation, $\Delta\theta$ (deg.)	0.024	0.014	0.004	0
$\Delta\theta$ /HPBW (%)	1.62	0.93	0.26	0
Maximum SLL (dB)	-9.54	-12.74	-13.05	-13.12
Directivity loss (dB)	0.88	0.22	0.053	0.013

The theoretical maximum SLL is –13.26 dB

Table 16 ***Averages of scan angle deviation, maximum SLL and directivity loss over scan angle for 110-element linear array with 2- to 5-bit phase shifter***

NUMBER OF PHASE SHIFTER BITS	2 BITS	3 BITS	4 BITS	5 BITS
Scan angle deviation, $\Delta\theta$ (deg.)	0.023	0.007	0.004	0
$\Delta\theta$ /HPBW (%)	2.01	0.53	0.35	0
Maximum SLL (dB)	-9.53	-12.93	-13.06	-13.17
Directivity loss (dB)	0.91	0.21	0.054	0.013

The theoretical maximum SLL is –13.26 dB

Table 17 ***Averages of scan angle deviation, maximum SLL and directivity loss over scan angle for 115-element linear array with 2- to 5-bit phase shifter***

NUMBER OF PHASE SHIFTER BITS	2 BITS	3 BITS	4 BITS	5 BITS
Scan angle deviation, $\Delta\theta$ (deg.)	0.013	0.009	0.002	0
$\Delta\theta$ /HPBW (%)	1.17	0.78	0.19	0
Maximum SLL (dB)	-9.62	-12.93	-13.08	-13.16
Directivity loss (dB)	0.88	0.22	0.053	0.013

The theoretical maximum SLL is –13.26 dB

Table 18 ***Averages of scan angle deviation, maximum SLL and directivity loss over scan angle for 128-element linear array with 2- to 5-bit phase shifter***

NUMBER OF PHASE SHIFTER BITS	2 BITS	3 BITS	4 BITS	5 BITS
Scan angle deviation, $\Delta\theta$ (deg.)	0.017	0.002	0.003	0
$\Delta\theta$ /HPBW (%)	1.77	0.22	0.31	0
Maximum SLL (dB)	-9.41	-13.03	-13.07	-13.19
Directivity loss (dB)	0.90	0.22	0.054	0.013

The theoretical maximum SLL is –13.26 dB

Annex 4 Equations of line and conics in the polar co-ordinate system

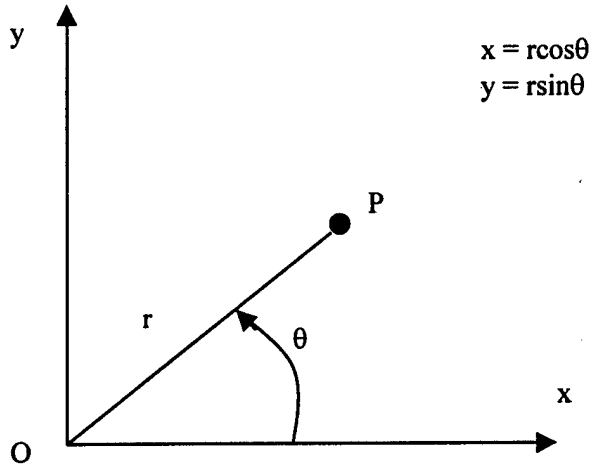

Figure 31: Cartesian and polar co-ordinate systems

Equation of a line

The general equation of a line in the two dimensional Cartesian co-ordinate system is expressed by

$$ax + by + c = 0 \qquad \textit{(eq. 24)}$$

Normalise the equation, that is make the sum of the squares of the coefficients of x and y equal to unity.

$$\left[\frac{a}{\sqrt{a^2+b^2}}\right]^2 + \left[\frac{b}{\sqrt{a^2+b^2}}\right]^2 = 1 \qquad \textit{(eq. 25)}$$

The equation of the line becomes

$$\frac{a}{\sqrt{a^2+b^2}}x + \frac{b}{\sqrt{a^2+b^2}}y + \frac{c}{\sqrt{a^2+b^2}} = 0 \qquad \textit{(eq. 26)}$$

The new coefficient of x and y can be respectively interpreted as the values of the cosine and sine of an angle α. The previous equation becomes

$$x\cos\alpha + y\sin\alpha + \frac{c}{\sqrt{a^2+b^2}} = 0 \qquad \textit{(eq. 27)}$$

Considering the Cartesian to polar transformation, it comes

$$r\cos\theta\cos\alpha + r\sin\vartheta\sin\alpha + r_o = 0 \quad \text{with } r_o = \frac{c}{\sqrt{a^2+b^2}} \qquad \textit{(eq. 28)}$$

$$\text{or} \quad r = -\frac{r_o}{\cos(\theta-\alpha)} \qquad \textit{(eq. 29)}$$

Equation of conics [8]

Conics can have different expressions, in either Cartesian and polar co-ordinate systems [8]. In the polar co-ordinate system, the equation of the conics referred to a focus as pole is

$$r = \frac{p}{1+\varepsilon\cos(\theta-\alpha)} \qquad \textit{(eq. 30)}$$

where ε is a positive number.

Different cases occur.

- If $\varepsilon > 1$, the conic is an hyperbola,
- If $\varepsilon = 1$, the conic is a parabola,
- If $0 < \varepsilon < 1$, the conic is an ellipse, and
- If $\varepsilon = 0$, the conic is a circle.

List of symbols/abbreviations/acronyms/initialisms

AF	Array Factor
DND	Department of National Defence
GL	Grating Lobe
HPBW	Half-Power Beam Width
QL	Quantisation Lobe
RMS	Root Mean Square
SLL	Side Lobe Level

DOCUMENT CONTROL DATA

(Security classification of title, body of abstract and indexing annotation must be entered when the overall document is classified)

1. ORIGINATOR (the name and address of the organization preparing the document. Organizations for whom the document was prepared, e.g. Establishment sponsoring a contractor's report, or tasking agency, are entered in section 8.)

Defence Research Establishment Ottawa
Department of National Defence
Ottawa, ON Canada K1A 0Z4

2. SECURITY CLASSIFICATION (overall security classification of the document, including special warning terms if applicable)

UNCLASSIFIED

3. TITLE (the complete document title as indicated on the title page. Its classification should be indicated by the appropriate abbreviation (S,C or U) in parentheses after the title.)

Graphical investigation of quantisation effects of phase shifters on array patterns (U)

4. AUTHORS (Last name, first name, middle initial)

Clénet, M., Morin, G.A.

5. DATE OF PUBLICATION (month and year of publication of document)

December 2000

6a. NO. OF PAGES (total containing information. Include Annexes, Appendices, etc.)

xii + 64

6b. NO. OF REFS (total cited in document)

8

7. DESCRIPTIVE NOTES (the category of the document, e.g. technical report, technical note or memorandum. If appropriate, enter the type of report, e.g. interim, progress, summary, annual or final. Give the inclusive dates when a specific reporting period is covered.)

DREO Technical Report

8. SPONSORING ACTIVITY (the name of the department project office or laboratory sponsoring the research and development. Include the address.)

9a. PROJECT OR GRANT NO. (if appropriate, the applicable research and development project or grant number under which the document was written. Please specify whether project or grant)

5ca12

9b. CONTRACT NO. (if appropriate, the applicable number under which the document was written)

10a. ORIGINATOR'S DOCUMENT NUMBER (the official document number by which the document is identified by the originating activity. This number must be unique to this document.)

DREO Technical Report No. 2000- 092

10b. OTHER DOCUMENT NOS. (Any other numbers which may be assigned this document either by the originator or by the sponsor)

11. DOCUMENT AVAILABILITY (any limitations on further dissemination of the document, other than those imposed by security classification)

(x) Unlimited distribution
( ) Distribution limited to defence departments and defence contractors; further distribution only as approved
( ) Distribution limited to defence departments and Canadian defence contractors; further distribution only as approved
( ) Distribution limited to government departments and agencies; further distribution only as approved
( ) Distribution limited to defence departments; further distribution only as approved
( ) Other (please specify):

12. DOCUMENT ANNOUNCEMENT (any limitation to the bibliographic announcement of this document. This will normally correspond to the Document Availability (11). However, where further distribution (beyond the audience specified in 11) is possible, a wider announcement audience may be selected.)

Full unlimited announcement

UNCLASSIFIED
SECURITY CLASSIFICATION OF FORM

13. ABSTRACT (a brief and factual summary of the document. It may also appear elsewhere in the body of the document itself. It is highly desirable that the abstract of classified documents be unclassified. Each paragraph of the abstract shall begin with an indication of the security classification of the information in the paragraph (unless the document itself is unclassified) represented as (S), (C), or (U). It is not necessary to include here abstracts in both official languages unless the text is bilingual).

This document presents graphical investigations of the array factor of phased arrays with digital phase shifters. A software program based on basic antenna array theory has been developed in Matlab to obtain the main array characteristics (array factor and directivity). The array factors of linear arrays of different sizes with different types of phase shifters have been studied as a function of the number of bits and the frequency. Unconventional two-dimensional colour graphical representations are used to identify some characteristics of the array factor of arrays with digital phase shifters that can not be so clearly and quickly visualised with conventional graphical representations. Particularly, the effects of quantisation on the array factor for arrays of different sizes and for phase shifters with different numbers of bits, over scanning and frequency ranges, are shown using this representation. Numerous data are also provided.

14. KEYWORDS, DESCRIPTORS or IDENTIFIERS (technically meaningful terms or short phrases that characterize a document and could be helpful in cataloguing the document. They should be selected so that no security classification is required. Identifiers such as equipment model designation, trade name, military project code name, geographic location may also be included. If possible keywords should be selected from a published thesaurus. e.g. Thesaurus of Engineering and Scientific Terms (TEST) and that thesaurus-identified. If it is not possible to select indexing terms which are Unclassified, the classification of each should be indicated as with the title.)

array factor
linear array
phased array